



Measurement of the jet radius and transverse momentum dependence of inclusive jet suppression in lead–lead collisions at $\sqrt{s_{\text{NN}}} = 2.76$ TeV with the ATLAS detector[☆]

ATLAS Collaboration*

ARTICLE INFO

Article history:

Received 9 August 2012
Received in revised form 28 December 2012
Accepted 14 January 2013
Available online 21 January 2013
Editor: D.F. Geesaman

Keywords:
LHC
ATLAS
Heavy ion
Jets

ABSTRACT

Measurements of inclusive jet suppression in heavy ion collisions at the LHC provide direct sensitivity to the physics of jet quenching. In a sample of lead–lead collisions at $\sqrt{s_{\text{NN}}} = 2.76$ TeV corresponding to an integrated luminosity of approximately $7 \mu\text{b}^{-1}$, ATLAS has measured jets with a calorimeter system over the pseudorapidity interval $|\eta| < 2.1$ and over the transverse momentum range $38 < p_{\text{T}} < 210 \text{ GeV}$. Jets were reconstructed using the anti- k_t algorithm with values for the distance parameter that determines the nominal jet radius of $R = 0.2, 0.3, 0.4$ and 0.5 . The centrality dependence of the jet yield is characterized by the jet “central-to-peripheral ratio,” R_{CP} . Jet production is found to be suppressed by approximately a factor of two in the 10% most central collisions relative to peripheral collisions. R_{CP} varies smoothly with centrality as characterized by the number of participating nucleons. The observed suppression is only weakly dependent on jet radius and transverse momentum. These results provide the first direct measurement of inclusive jet suppression in heavy ion collisions and complement previous measurements of dijet transverse energy imbalance at the LHC.

© 2013 CERN. Published by Elsevier B.V. Open access under CC BY-NC-ND license.

1. Introduction

Collisions of lead ions at the LHC are expected to create strongly interacting matter at the highest temperatures ever produced in the laboratory [1]. This matter may be deconfined with a high density of unscreened colour charges. High transverse momentum (p_{T}) quarks and gluons generated by hard-scattering processes have long been considered an important tool for probing the properties of the matter created in ultra-relativistic nuclear collisions. The energy loss of the partons propagating through the matter may provide direct sensitivity to the colour charge density and to the transport properties of the matter [2–4]. Indirect observations of substantial parton energy loss or “jet quenching” via suppressed single high- p_{T} hadron yields [5–8] and disappearance of the dijet contribution to di-hadron correlations [9,10] have contributed to the conclusion that Au + Au collisions at RHIC produce a quark-gluon plasma [11,12]. Observations of highly asymmetric dijets in central Pb + Pb collisions at the LHC [13–15] can be understood in the context of “differential” jet quenching, where one parton produced from an initial hard-scattering loses significantly more energy than the other, possibly as a result of different path lengths of the partons in the matter [16]. However, the asymmetry is not sensitive to situations where the two jets in a dijet pair lose com-

parable amounts of energy, so other measurements are required to probe “inclusive” jet quenching.

The inclusive, per-event jet production rate provides such a measurement. Energy loss of the parent partons in the created matter may reduce or “suppress” the rate for producing jets at a given transverse momentum. Such energy loss is expected to increase with medium temperature and with increasing path length of the parton in the medium [17]. As a result, there should be more suppression in central Pb + Pb collisions, which have nearly complete overlap between the incident nuclei, and little or no suppression in peripheral collisions where the nuclei barely overlap. In the absence of energy loss, the jet production rate is expected to vary with Pb + Pb collision centrality approximately in proportion to N_{coll} , the number of nucleon–nucleon collisions that take place during a single Pb + Pb collision. The jet suppression may be quantified using the central-to-peripheral ratio, R_{CP} , the ratio of the per-event jet yields divided by the number of nucleon–nucleon collisions in a given centrality bin to the same quantity in a peripheral centrality bin. The quantity, R_{CP} , has the advantage that potentially large systematic uncertainties, especially those arising from systematic errors on the jet energy scale, largely cancel when evaluating the ratios of jet spectra within the same data set. The variation of the suppression with jet transverse momentum and with collision centrality will depend both on the energy loss mechanism and on the experimental definition of the jet. In the case of radiative energy loss, jet energies can be reduced by greater “out-of-cone” radiation, which should be more severe for

* E-mail address: atlas.publications@cern.ch.

smaller jet radii [18–20]. Naively, collisional energy loss would result in a suppression that is independent of radius. However recent calculations suggest that collisional processes can also contribute to jet broadening [21]. A measurement of the radius dependence of jet suppression could further clarify the roles of radiative and collisional energy loss in jet quenching.

This Letter presents measurements of the inclusive jet R_{CP} in $\text{Pb} + \text{Pb}$ collisions at a nucleon-nucleon centre-of-mass energy of $\sqrt{s_{\text{NN}}} = 2.76$ TeV using data collected during 2010 corresponding to an integrated luminosity of approximately $7 \mu\text{b}^{-1}$. Results are presented for jets reconstructed from energy deposits measured in the ATLAS calorimeters using the anti- k_t jet-finding algorithm [22]. The anti- k_t reconstruction was performed separately for four different values of the anti- k_t distance parameter, R , that specifies the nominal radius of the reconstructed jets, $R = 0.2, 0.3, 0.4$ and 0.5 . For the remainder of the Letter the term “radius” will refer to the distance parameter, R . The jet energy is functionally defined to be the total energy within the jet clustering algorithm above an uncorrelated underlying event. This jet definition may include medium response with is correlated with the jet. The underlying event contribution to each jet was subtracted on a per-jet basis, and the R_{CP} values were calculated after unfolding the jet spectra for distortions due to intrinsic jet resolution and underlying event fluctuations.

2. Experimental setup and trigger

The measurements presented here were performed using the ATLAS calorimeter, inner detector, trigger, and data acquisition systems [23]. The ATLAS calorimeter system consists of a liquid argon (LAr) electromagnetic (EM) calorimeter covering $|\eta| < 3.2$, a steel-scintillator sampling hadronic calorimeter covering $|\eta| < 1.7$, a LAr hadronic calorimeter covering $1.5 < |\eta| < 3.2$, and two LAr electromagnetic and hadronic forward calorimeters (FCal) covering $3.2 < |\eta| < 4.9$.¹ The hadronic calorimeter granularities or cell sizes in $\Delta\eta \times \Delta\phi$ are 0.1×0.1 for $|\eta| < 2.5$ and 0.2×0.2 for $2.5 < |\eta| < 4.9$.² The EM calorimeters are longitudinally segmented into three compartments with an additional pre-sampler layer. The EM calorimeter has a granularity that varies with layer and pseudorapidity, but which is generally much finer than that of the hadronic calorimeter. The middle sampling layer, which typically has the largest energy deposit in EM showers, has a $\Delta\eta \times \Delta\phi$ granularity of 0.025×0.025 over $|\eta| < 2.5$.

Charged particles associated with the calorimeter jets were measured over the pseudorapidity interval $|\eta| < 2.5$ using the inner detector [24]. The inner detector is composed of silicon pixel detectors in the innermost layers, followed by silicon microstrip detectors and a straw-tube tracker, all immersed in a 2 T axial magnetic field provided by a solenoid. Minimum bias $\text{Pb} + \text{Pb}$ collisions were identified using measurements from the zero-degree calorimeters (ZDCs) and the minimum-bias trigger scintillator (MBTS) counters. The ZDCs are located symmetrically at $z = \pm 140$ m and cover $|\eta| > 8.3$. In $\text{Pb} + \text{Pb}$ collisions the ZDCs primarily measure “spectator” neutrons – neutrons from the incident nuclei that do not interact hadronically. The MBTS measures charged particles over $2.1 < |\eta| < 3.9$ using two sets of counters

¹ ATLAS uses a right-handed coordinate system with its origin at the nominal interaction point (IP) in the centre of the detector and the z -axis along the beam pipe. The x -axis points from the IP to the centre of the LHC ring, and the y -axis points upward. Cylindrical coordinates (r, ϕ) are used in the transverse plane, ϕ being the azimuthal angle around the beam pipe. The pseudorapidity is defined in terms of the polar angle θ as $\eta = -\ln \tan(\theta/2)$.

² An exception is the third (outermost) sampling layer, which has a segmentation of 0.2×0.1 up to $|\eta| = 1.7$.

Table 1

Results of Glauber model evaluation of $\langle N_{\text{part}} \rangle$ and associated errors, $\langle N_{\text{coll}} \rangle$, the N_{coll} ratios, R_{coll} , and fractional errors on R_{coll} for the centrality bins included in this analysis.

Centrality	$\langle N_{\text{part}} \rangle$	$\langle N_{\text{coll}} \rangle$	R_{coll}
0–10%	356 ± 2	1500 ± 115	57 ± 6
10–20%	261 ± 4	923 ± 68	35 ± 4
20–30%	186 ± 4	559 ± 41	21 ± 2
30–40%	129 ± 4	322 ± 24	12 ± 1
40–50%	86 ± 4	173 ± 14	6.5 ± 0.04
50–60%	53 ± 3	85 ± 8	3.2 ± 0.01
60–80%	23 ± 2	27 ± 4	1

placed at $z = \pm 3.6$ m. Events used in this analysis were selected for recording by the data acquisition system using a logical or of ZDC and MBTS coincidence triggers. The MBTS coincidence required at least one hit in each side of the detector, and the ZDC coincidence trigger required the summed pulse height from each calorimeter to be above a threshold set below the single neutron peak.

3. Event selection and centrality definition

In the offline analysis, $\text{Pb} + \text{Pb}$ collisions were required to have a primary vertex reconstructed from charged particle tracks with $p_{\text{T}} > 500$ MeV. The tracks were reconstructed from hits in the inner detector using the standard ATLAS track reconstruction algorithm [25] with settings optimized for the high hit density in heavy ion collisions [26]. Additional requirements of a ZDC coincidence, at least one hit in each MBTS counter, and a difference in times measured by the two sides of the MBTS detector of less than 3 ns were imposed. The combination of the ZDC and MBTS conditions and the primary vertex requirement efficiently eliminates both beam-gas interactions and photo-nuclear events [27]. These event selections yielded a total of 51 million minimum-bias $\text{Pb} + \text{Pb}$ events. Previous studies [26] indicate that the combination of trigger and offline requirements select minimum-bias hadronic $\text{Pb} + \text{Pb}$ collisions with an efficiency of $98 \pm 2\%$.

The centrality of $\text{Pb} + \text{Pb}$ collisions was characterized by $\Sigma E_{\text{T}}^{\text{FCal}}$, the total transverse energy measured in the forward calorimeters. The distribution of $\Sigma E_{\text{T}}^{\text{FCal}}$ was divided into intervals corresponding to successive 10% percentiles of the full centrality distribution after accounting for the missing 2% most peripheral events. A standard Glauber Monte Carlo analysis [28,29] was used to estimate the average number of participating nucleons, $\langle N_{\text{part}} \rangle$, and the average number of nucleon-nucleon collisions, $\langle N_{\text{coll}} \rangle$, for $\text{Pb} + \text{Pb}$ collisions in each of the centrality bins. The results are shown in Table 1. The R_{CP} measurements presented here use the 60–80% centrality bin as a common peripheral reference. The R_{CP} calculation requires the ratio, $R_{\text{coll}} \equiv \langle N_{\text{coll}} \rangle / \langle N_{\text{coll}}^{60-80} \rangle$, where $\langle N_{\text{coll}}^{60-80} \rangle$ is the average number of collisions in the 60–80% centrality bin. The R_{coll} uncertainties have been calculated by evaluating the changes in R_{coll} due to variations of the minimum-bias trigger efficiency, parameters of the Glauber calculation, and parameters in the modelling of the $\Sigma E_{\text{T}}^{\text{FCal}}$ distribution [26]. The R_{coll} values and uncertainties are also reported in Table 1.

4. Monte Carlo samples

Three Monte Carlo (MC) samples [30] were used for the analysis in this Letter. A total of 1 million simulated minimum-bias $\text{Pb} + \text{Pb}$ events were produced using version 1.38b of the HIJING event generator [31]. HIJING was run with default parameters except for the disabling of jet quenching. To simulate the effects of elliptic flow in $\text{Pb} + \text{Pb}$ collisions, a parameterized centrality-, η - and

p_T -dependent $\cos 2\phi$ modulation based on previous ATLAS measurements [26] was imposed on the particles after generation [32]. The detector response to the resulting HIJING events was evaluated using GEANT4 [33] configured with geometry and digitization parameters matching those of the 2010 Pb + Pb run.

An “MC overlay” data set, intended specifically for evaluating jet performance, was obtained by overlaying GEANT4-simulated $\sqrt{s_{NN}} = 2.76$ TeV pp hard-scattering events on the HIJING events described above. The pp events were obtained from the ATLAS MC09 tune [34] of the PYTHIA event generator [35]. One million PYTHIA hard-scattering events were generated for each of five intervals of \hat{p}_T , the transverse momentum of outgoing partons in the $2 \rightarrow 2$ hard-scattering, with boundaries 17, 35, 70, 140, 280 and 560 GeV. The pp events for each \hat{p}_T interval were overlaid on the same sample of HIJING events.

A smaller sample of “data overlay” events was produced by overlaying 150k GEANT4-simulated PYTHIA pp events onto 150k minimum-bias Pb + Pb data events recorded during the 2011 LHC Pb + Pb run. Due to the different detector conditions in the 2010 and 2011 runs, the data overlay events cannot provide the corrections required for this analysis. However, they provide a valuable test of the accuracy of HIJING in describing the underlying event.

5. Jet reconstruction

Calorimeter jets were reconstructed from $\Delta\eta \times \Delta\phi = 0.1 \times 0.1$ towers using the anti- k_t algorithm [22] in four-vector recombination mode with anti- k_t distance parameters $R = 0.2, 0.3, 0.4$ and 0.5. The tower energies were obtained by summing energies, calibrated at the electromagnetic energy scale [36], of all cells in all layers within the η and ϕ boundaries of the towers. Cells that span tower boundaries had their energy apportioned by the fraction of the cell contained within a given tower. The jet measurements presented here were obtained by performing the anti- k_t reconstruction on the towers prior to underlying event (UE) subtraction and then evaluating and subtracting the UE from each jet at the calorimeter cell level. The subtraction procedure calculates a per-event average UE energy density excluding contributions from jets and accounting for effects of elliptic flow modulation on the UE [37]. The UE estimation and subtraction was performed using a two-step procedure that was identical for all jet radii.

A first estimate of the UE average transverse energy density, $\rho_i(\eta)$, was evaluated in 0.1 intervals of η from all cells in each calorimeter layer, i , within the given η interval excluding those within “seed” jets. In the first subtraction step, the seeds are defined to be $R = 0.2$ jets containing at least one tower with $E_T > 3$ GeV and having a ratio of maximum tower transverse energy to average tower transverse energy, $E_T^{\max}/\langle E_T \rangle > 4$. Elliptic flow in Pb + Pb collisions can impose a $2v_2 \cos[2(\phi - \Psi_2)]$ modulation on the UE. Here, v_2 is the second coefficient in a Fourier decomposition of the azimuthal variation of the UE particle or energy density, and the event plane angle, Ψ_2 , determines the phase of the elliptic modulation. Standard techniques [26,37] were used to measure Ψ_2 ,

$$\Psi_2 = \frac{1}{2} \tan^{-1} \left(\frac{\sum_k w_k E_{Tk} \sin(2\phi_k)}{\sum_k w_k E_{Tk} \cos(2\phi_k)} \right), \quad (1)$$

where k runs over cells in the FCal, ϕ_k represents the cell azimuthal angle, and w_k represent per-cell weights empirically determined to ensure a uniform Ψ_2 distribution. An η -averaged v_2 was measured separately for each calorimeter layer according to

$$v_{2i} = \frac{\sum_{j \in i} E_{Tj} \cos[2(\phi_j - \Psi_2)]}{\sum_{j \in i} E_{Tj}}, \quad (2)$$

where j runs over all cells in layer i . The UE-subtracted cell transverse energies were calculated according to

$$E_{Tj}^{\text{sub}} = E_{Tj} - A_j \rho_i(\eta_j) (1 + 2v_{2i} \cos[2(\phi_j - \Psi_2)]), \quad (3)$$

where E_{Tj} , η_j , ϕ_j and A_j represent the cell E_T , η and ϕ positions, and area, respectively for cells, j , in layer i . The kinematics for $R = 0.2$ jets generated in this first subtraction step were calculated via a four-vector sum of all (assumed massless) cells contained within the jets using the E_T values obtained from Eq. (3).

The second subtraction step starts with the definition of a new set of seeds using a combination of $R = 0.2$ jets from the first subtraction step with $E_T > 25$ GeV and track jets (defined below) with $p_T > 10$ GeV. Using this new set of seeds, a new estimate of the UE, $\rho'_i(\eta)$, was calculated excluding cells within $\Delta R = 0.4$ of the new seed jets, where $\Delta R = \sqrt{(\eta_{\text{cell}} - \eta_{\text{jet}})^2 + (\phi_{\text{cell}} - \phi_{\text{jet}})^2}$. New v_{2i} values, v'_{2i} , were also calculated excluding all cells within $\Delta\eta = 0.4$ of any of the new seed jets. This exclusion largely eliminates distortions of the calorimeter v_2 measurement in events containing high- p_T jets. The background subtraction was then applied to the original cell energies using Eq. (3) but with ρ_i and v_{2i} replaced by the new values, $\rho'_i(\eta)$ and v'_{2i} . New jet kinematics were obtained for all jet radii from a four-momentum sum of cells within the jets using the subtracted cell transverse energies. Jets generated in this second subtraction step having $E_T > 20$ GeV were recorded for subsequent analysis.

A correction of typically a few per cent was applied to the reconstructed jets to account for incomplete exclusion of towers within jets from the UE estimate due, for example, to differences in direction between the seeds and the final jets. This correction was validated by applying the full heavy ion jet reconstruction procedure to 2.76 TeV pp data collected by ATLAS in March 2011. The reconstructed jets were compared, jet-by-jet, to those obtained from the pp jet reconstruction procedure. After this last correction for incomplete exclusion of jets from the background, the energy scales of the heavy ion and pp reconstruction procedures agreed to better than 1% for $E_T > 25$ GeV. A final correction depending on the jet η , E_T , and R was applied to obtain the correct hadronic energy scale for the reconstructed jets. The calibration constants were derived separately for the four jet radii using the same procedure applied to pp jet measurements [36].

In addition to the calorimeter jet reconstruction, track jets were reconstructed using the anti- k_t algorithm with $R = 0.4$ from charged tracks that have a good match to the primary vertex and that have $p_T > 4$ GeV. This threshold suppresses contributions of the UE to the track jet measurement. Specifically, an $R = 0.4$ track jet has an estimated likelihood of including an uncorrelated $p_T > 4$ GeV charged track of less than 4% in the 0–10% centrality bin. The single track reconstruction efficiency is $\approx 80\%$, approximately independent of centrality.

The fluctuating UE in Pb + Pb collisions can potentially produce reconstructed jets that do not originate from hard-scattering processes. In the remainder of this Letter such jets are referred to as “underlying event jets” or UE jets. A requirement that calorimeter jets match at least one track jet with $p_T > 7$ GeV or an EM cluster reconstructed from cells in the electromagnetic calorimeter [38] with $p_T > 7$ GeV was applied to exclude UE jets. The matching criterion for both track jets and EM clusters is that they lie within $\Delta R = 0.2$ of the jet. Applying this matching requirement provides a factor of about 50 rejection against UE jets while inducing an additional p_T -dependent inefficiency in the jet measurement. To accommodate the use of track jets in the UE jet rejec-

Table 2

Total number of jets in the data set with $p_T > 40$ GeV and $p_T > 100$ GeV in the 0–10% and 60–80% centrality bins after all event selection criteria, UE jet rejection, and the $|\eta| < 2.1$ cut have been applied.

R	$p_T > 40$ GeV		$p_T > 100$ GeV	
	0–10%	60–80%	0–10%	60–80%
0.2	112 333	8068	2308	162
0.3	287 153	12629	3534	222
0.4	543 444	15964	4974	277
0.5	710 158	18573	7586	307

tion, the jet measurements presented here have been restricted to $|\eta| < 2.1$. The total number of jets above p_T thresholds of 40 GeV and 100 GeV in the data sample after event selection, UE jet rejection, and the $|\eta| < 2.1$ cut have been applied is shown in Table 2 for the most central and peripheral bins.

6. Performance of the jet reconstruction

The primary evaluation of the combined performance of the ATLAS detector and the analysis procedures described above in measuring unquenched jets was obtained using the MC overlay sample. In that MC sample, the kinematics of the reference PYTHIA generator-level jets (hereafter called “truth jets”) were reconstructed from PYTHIA final-state particles for $R = 0.2, 0.3, 0.4$ and 0.5 using the same techniques as applied in pp analyses [36]. Separately, the presence and approximate kinematics of HIJING-generated jets were obtained by running $R = 0.4$ anti- k_t reconstruction on final-state HIJING particles having $p_T > 4$ GeV. Accidental overlap of jets from unrelated hard-scattering processes may occur at non-negligible rates in the data due to the geometric enhancement of hard-scattering rates in Pb + Pb collisions. However, for the purposes of this Letter, the resulting combined jets are considered part of the physical jet spectrum and not a result of UE fluctuations. Then, to prevent the overlap of PYTHIA and HIJING jets from distorting the jet performance evaluated relative

to PYTHIA truth jets, all PYTHIA truth jets within $\Delta R = 0.8$ of a $p_T > 10$ GeV HIJING jet were excluded from the analysis.

Following reconstruction of the overlaid MC events using the same algorithms that were applied to the data, PYTHIA truth jets passing the HIJING-jet exclusion were matched to the closest reconstructed jet of the same R value within $\Delta R = 0.2$. The resulting matched jets were used to evaluate the jet energy resolution (JER) and the jet energy scale (JES). The jet reconstruction efficiency was defined as the fraction of truth jets for which a matching reconstructed jet is found. The efficiency was evaluated both prior to (ε) and following (ε') UE jet rejection. For all three performance measurements, the different \hat{p}_T MC overlay samples were combined using a weighting based on the PYTHIA cross-sections for each \hat{p}_T range.

Fig. 1 shows a summary of the ATLAS Pb + Pb jet reconstruction performance for $R = 0.2$ and $R = 0.4$ jets in central (0–10%) and peripheral (60–80%) collisions. The (fractional) JER was characterized by $\sigma[\Delta E_T]/E_T^{\text{truth}}$, where $\sigma[\Delta E_T]$ is the standard deviation of the $\Delta E_T \equiv E_T^{\text{rec}} - E_T^{\text{truth}}$ distribution and where E_T^{rec} and E_T^{truth} are the reconstructed and truth jet E_T values, respectively. The JES offset or “closure” was evaluated from the mean fractional energy shift, $\langle \Delta E_T \rangle/E_T^{\text{truth}}$.

The JER was found to be well described by a quadrature sum of three terms,

$$\frac{\sigma[\Delta E_T]}{E_T^{\text{truth}}} = \frac{a}{\sqrt{E_T^{\text{truth}}}} \oplus \frac{b}{E_T^{\text{truth}}} \oplus c, \quad (4)$$

where a and c represent the usual sampling and constant contributions to calorimeter resolution. The term containing b describes the contribution of underlying event fluctuations, which do not depend on jet E_T . Results of fitting the E_T dependence of the JER according to Eq. (4), using methods described below, are shown with curves in Fig. 1.

The jet reconstruction efficiency decreases with decreasing jet E_T for $E_T \lesssim 50$ GeV. The decrease starts at larger E_T and decreases more rapidly for larger jet radii and in more central col-

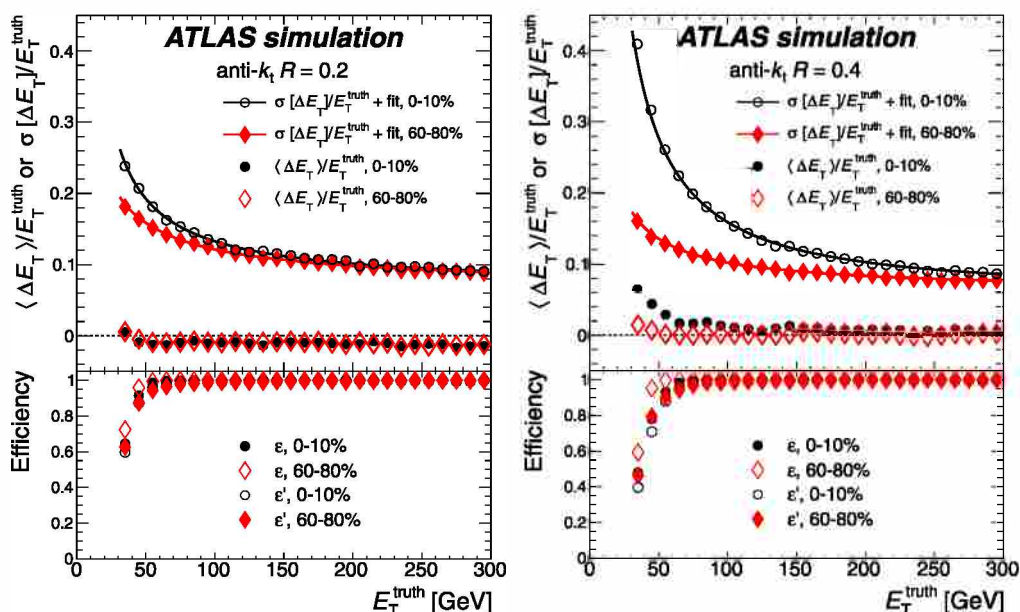


Fig. 1. Results of MC evaluation of jet reconstruction performance in 0–10% and 60–80% collisions as a function of truth jet E_T for $R = 0.2$ (left) and $R = 0.4$ (right) jets. Top: jet energy resolution $\sigma[\Delta E_T]/E_T^{\text{truth}}$ and jet energy scale closure, $\langle \Delta E_T \rangle/E_T^{\text{truth}}$. Solid curves show parameterizations of the JER using Eq. (4). Bottom: Efficiencies, ε and ε' , for reconstructing jets before and after application of UE jet removal (see text for explanation), respectively.

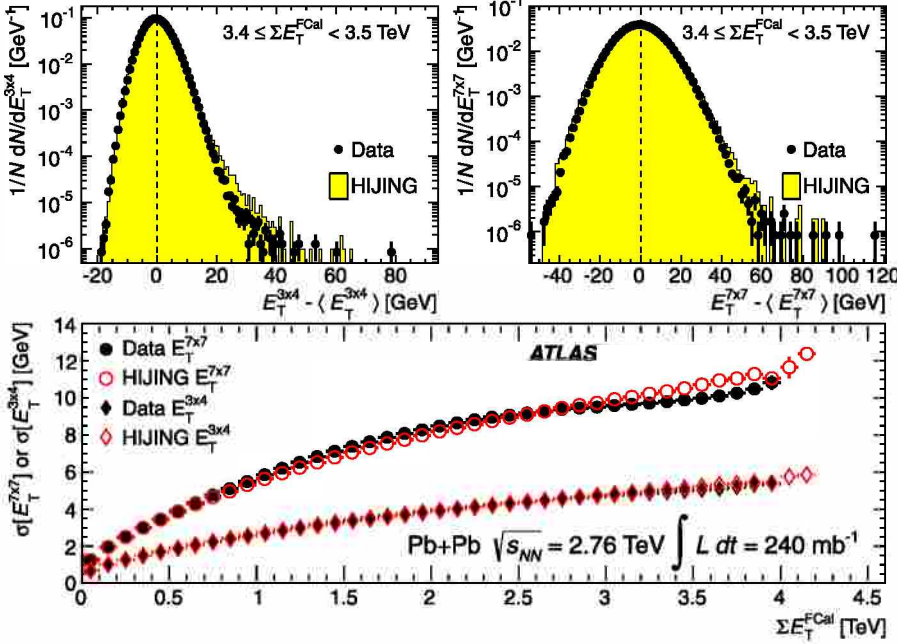


Fig. 2. Top: Representative distributions of $E_T^{3\times 4} - \langle E_T^{3\times 4} \rangle$ (left) and $E_T^{7\times 7} - \langle E_T^{7\times 7} \rangle$ (right) (see text for definitions) for data (points) and MC (filled histogram) for Pb + Pb collisions with $3.4 \leq \Sigma E_T^{\text{Cal}} < 3.5 \text{ TeV}$. The vertical lines indicate $E_T^{3\times 4} - \langle E_T^{3\times 4} \rangle = 0$ and $E_T^{7\times 7} - \langle E_T^{7\times 7} \rangle = 0$. Bottom: Standard deviations of the $E_T^{3\times 4}$ and $E_T^{7\times 7}$ distributions, $\sigma[E_T^{3\times 4}]$ and $\sigma[E_T^{7\times 7}]$, respectively, in data and HIJING MC sample as a function of ΣE_T^{Cal} .

lisions. The inefficiency results primarily from the finite JER which causes jets with $E_T^{\text{truth}} > 20 \text{ GeV}$ to be measured with $E_T^{\text{rec}} < 20 \text{ GeV}$. The UE jet rejection causes an additional loss of jets but in a manner that reduces the centrality dependence of the inefficiency.

The accuracy of the MC overlay studies described above was evaluated using the data overlay sample analyzed using the same procedures that were applied to the MC overlay sample. The analysis yielded results for the JER, JES, and efficiency consistent with the MC overlay sample, although the JER in the data overlay sample was found to be slightly better than in the MC overlay sample. The JES in the data overlay sample was found to agree between peripheral and central collisions to better than 1% for $R = 0.4$ jets, and the reconstruction efficiency was found to differ by less than 5% on the rise of the efficiency curve.

A data-driven check of the HIJING description of UE fluctuations was performed by evaluating distributions of EM-scale summed E_T in rectangular groups of towers within the interval $|\eta| < 2.8$. The groups were chosen to match the areas of jets used in this analysis: 3×4 and 7×7 for $R = 0.2$ and $R = 0.4$ jets, respectively. No attempt was made to exclude jets from the fluctuation analysis. The distributions of $E_T^{3\times 4}$ and $E_T^{7\times 7}$, the ΣE_T for 3×4 and 7×7 groups of towers, are shown in Fig. 2 for a narrow range of ΣE_T^{Cal} , $3.4 \leq \Sigma E_T^{\text{Cal}} < 3.5 \text{ TeV}$, that lies within the 0–1% centrality interval. These distributions have mean values, $\langle E_T^{3\times 4} \rangle = 26 \text{ GeV}$ and $\langle E_T^{7\times 7} \rangle = 105 \text{ GeV}$, subtracted and, thus, in principle represent the distribution of the residual contributions of the UE to jet energies after subtraction. However, the high tails of the distributions can be attributed to the presence of jets, which are not part of the UE. The corresponding distributions obtained from the HIJING MC sample, but with $\langle E_T^{3\times 4} \rangle$ and $\langle E_T^{7\times 7} \rangle$ obtained from data, are shown in Fig. 2 with filled histograms.

The shapes of the MC and data distributions in Fig. 2 (top) are very similar, but the MC result slightly over-predicts the positive fluctuations for all collision centralities. In central collisions the MC result also slightly over-predicts the size of negative fluctua-

tions. In contrast, for non-central collisions (not shown here) the data has a broader distribution of negative fluctuations than the MC sample. These observations are demonstrated by Fig. 2 (bottom) which shows the standard deviations of the $E_T^{3\times 4}$ and $E_T^{7\times 7}$ distributions, $\sigma[E_T^{3\times 4}]$ and $\sigma[E_T^{7\times 7}]$, as a function of ΣE_T^{Cal} , obtained from both the data and the MC sample. The data and MC distributions have similar trends, but the MC $\sigma[E_T^{3\times 4}]$ and $\sigma[E_T^{7\times 7}]$ values are larger in central collisions by 2.5% and 5%, respectively. In non-central collisions, the broader spectrum of negative fluctuations in the data causes $\sigma[E_T^{3\times 4}]$ and $\sigma[E_T^{7\times 7}]$ to exceed the corresponding quantity in the HIJING MC sample by approximately the same percentages.

Consistency between the results of the fluctuation analysis and the evaluation of the JER described above has been established by fitting the E_T dependence of the JER with the functional form given by Eq. (4) with fixed b values obtained from the fluctuation analysis. The b values for a given jet radius were determined by taking the standard deviation of the ΣE_T distribution for the corresponding tower group averaged over centrality and corrected to the hadronic energy scale. The resulting b values for $R = 0.2$ (0.4) jets are 5.62 (12.45) GeV and 1.15 (2.58) GeV for the 0–10% and 60–80% centrality bins respectively. The parameters a and c obtained from the fits are found to be independent of centrality within fit uncertainties, as expected, and to have values $a = 1.0$ (0.8), $c = 0.07$ (0.06) for $R = 0.2$ (0.4) jets with E_T expressed in GeV. The accuracy of the fits in describing the E_T dependence of the JER is demonstrated by the curves showing results for $R = 0.2$ and $R = 0.4$ jets in Fig. 1.

The contribution of UE jets to the measured jet spectrum after UE jet rejection is estimated to be $\lesssim 3\%$ approximately independent of jet p_T for $40 < p_T < 60 \text{ GeV}$ and less than 1% for $p_T > 60 \text{ GeV}$. This estimate was obtained by evaluating the rate of reconstructed jets in the HIJING MC sample which were not matched to HIJING truth jets and correcting for missing truth jets due to the $p_T > 4 \text{ GeV}$ requirement applied in the HIJING truth jet reconstruction.

7. Jet spectra and unfolding

Though jet reconstruction performance is naturally evaluated in terms of jet E_T , the physics measurements in this Letter were performed as a function of p_T directly calculated from the jet four-momentum. The typical masses of the jets are sufficiently small that $E_T \approx p_T$ holds over the range of measured p_T for all jet radii. The measured p_T spectra of reconstructed jets passing UE jet rejection and having $|\eta| < 2.1$ were evaluated for each centrality bin using logarithmic p_T bins spanning the range $38 < p_T < 210$ GeV. The correlations within and between p_T bins arising from multi-jet events were quantified by the covariance, C_{ij} , between the number of jets measured in two bins, i and j . The measured R_{CP} was calculated as

$$R_{CP}^{\text{meas}}(p_T)|_{\text{cent}} = \frac{1}{R_{\text{coll}}^{\text{cent}}} \left(\frac{\frac{N_{\text{jet}}^{\text{cent}}(p_T)}{N_{\text{evt}}^{\text{cent}}}}{\frac{N_{\text{jet}}^{60-80}(p_T)}{N_{\text{evt}}^{60-80}}} \right), \quad (5)$$

where $N_{\text{jet}}^{\text{cent}}$ represents the measured jet yield in a given p_T and centrality bin, and $N_{\text{evt}}^{\text{cent}}$ and N_{evt}^{60-80} are the number of Pb + Pb collisions within the chosen and peripheral reference centrality intervals, respectively. Results for $R_{CP}^{\text{meas}}|_{0-10}$ obtained from the measured spectra are shown in Fig. 3 for $R = 0.2$ and $R = 0.4$ jets. The $R_{CP}^{\text{meas}}|_{0-10}$ for $R = 0.2$ jets is approximately equal to 0.5 over the measured p_T range. The $R_{CP}^{\text{meas}}|_{0-10}$ for $R = 0.4$ and $R = 0.2$ jets are consistent for $p_T > 120$ GeV, but at lower p_T , the $R = 0.4$ $R_{CP}^{\text{meas}}|_{0-10}$ increases relative to the $R = 0.2$ values. The difference between $R = 0.2$ and $R = 0.4$ $R_{CP}^{\text{meas}}|_{0-10}$ values can be mostly attributed to the difference in the size of the UE fluctuations for $R = 0.2$ and $R = 0.4$ jets shown in Fig. 1. The larger JER for $R = 0.4$ jets produces greater upward migration on the steeply falling jet p_T spectrum in central collisions than in peripheral collisions, thus enhancing the measured R_{CP} . The drop in the $R = 0.4$ $R_{CP}^{\text{meas}}|_{0-10}$ at low p_T is due to the decrease in jet reconstruction efficiency between 60–80% and 0–10% centrality bins which, as noted above, largely results from the worse JER in central collisions.

To remove the effects of the bin migration, the jet spectra were unfolded using the singular value decomposition (SVD) technique [39] as implemented in `RootUnfold` [40]. The MC overlay samples were used to populate a response matrix, \mathbf{A} , which describes the transformation of the true jet spectrum, \mathbf{x} , to the observed spectrum, \mathbf{b} , according to $\mathbf{b} = \mathbf{Ax}$. The truth and reconstructed jet p_T were obtained from the MC overlay sample using the methods described in Sections 6 and 5, respectively, and the selection and matching of truth and reconstructed jet pairs was performed as described in Section 6. Using the weighting method suggested in Ref. [39], the unfolded spectrum is expressed as a set of weights \mathbf{w} multiplying the input spectrum (x_{ini}) used to produce \mathbf{A} . The SVD method expresses the solution for \mathbf{w} in terms of a least-square minimization problem that includes a prescription for regularizing the amplification of statistical fluctuations of the data that would result from the direct inversion of \mathbf{A} . The regularization is controlled by a parameter τ such that contributions from singular values s_k of the unfolding matrix with $s_k < \tau$ are suppressed. Inclusion of the p_T -dependent reconstruction efficiency in the response was found to strongly affect the spectrum of singular values of the matrix defining the SVD problem, so the efficiency correction was applied separately following the unfolding. The spectrum of MC truth jets was reweighted to provide a smooth, power-law initial spectrum, $x_{\text{ini}} \propto \varepsilon'(p_T)/p_T^n$, where the power index was chosen to be $n = 5$. An analysis of the optimal regularization in the SVD unfolding following the methods of Ref. [39] indicated that a regularization parameter fixed by the fifth singular value ($\tau = s_5^2$)

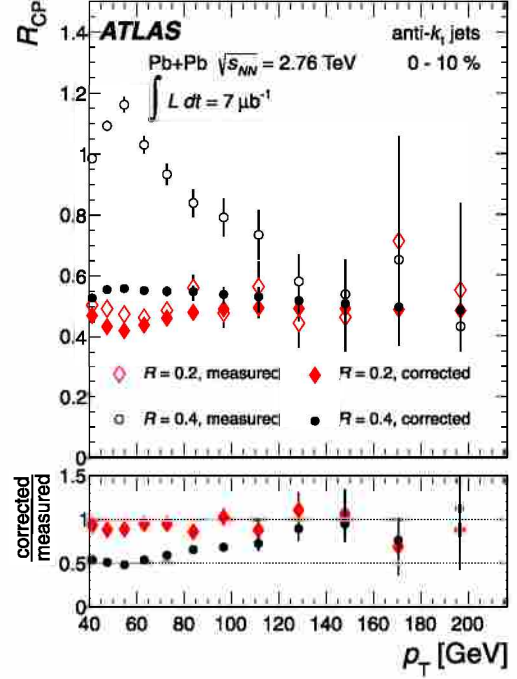


Fig. 3. Top: Measured and corrected R_{CP} values for the 0–10% centrality bin as a function of jet p_T for $R = 0.4$ and $R = 0.2$ jets. Bottom: Ratio of corrected to measured R_{CP} values for both jet radii. The error bars on the points represent statistical uncertainties only.

of the SVD matrix was appropriate for all centralities and all R values. The statistical uncertainties in the SVD unfolding due to statistical errors on the input spectrum were evaluated using the pseudo-experiment technique with 1000 separate stochastic variations of the input spectrum based on the full covariance matrix. The contributions of statistical fluctuations in the response matrix, \mathbf{A} , were similarly evaluated using an equal number of stochastic variations of the response matrix. The two contributions to the statistical uncertainty were combined in quadrature.

Potential biases in the unfolding procedure were evaluated using two different methods. Each unfolded spectrum was re-folded with its corresponding response matrix and compared to the measured spectrum for self-consistency. In general, regularization can introduce differences between re-folded and measured spectra on the scale of statistical uncertainties on the measured spectra, while over-regularization can produce larger, systematic differences. For all of the unfolded spectra, the re-folding procedure yielded a typical difference between measured and re-folded spectra comparable to the statistical uncertainties on the measured spectra. A separate check was performed by unfolding the reconstructed MC spectrum for each centrality bin and each jet radius and comparing to the original MC truth jet spectrum. For this purpose, the MC data sets were divided in half and reconstructed spectra and response matrices were generated separately from each set. The unfolded and truth MC jet spectra typically agreed to better than 2%, though for the 0–10% centrality bin and for $R = 0.4$ and 0.5 jets, differences as large as 5% were observed in the lowest p_T bins. These differences are covered by the unfolding systematic uncertainties described below.

The corrected R_{CP} was evaluated according to

$$R_{CP}(p_T)|_{\text{cent}} = \frac{1}{R_{\text{coll}}^{\text{cent}}} \left(\frac{\frac{\tilde{N}_{\text{jet}}^{\text{cent}}(p_T)}{\varepsilon' \text{cent} N_{\text{evt}}^{\text{cent}}}}{\frac{\tilde{N}_{\text{jet}}^{60-80}(p_T)}{\varepsilon' 60-80 N_{\text{evt}}^{60-80}}} \right), \quad (6)$$

where \bar{N}_{jet} represents the unfolded number of jets in the p_{T} bin, and $\varepsilon^{\text{cent}}$ and ε^{60-80} are the p_{T} -dependent jet reconstruction efficiencies after UE jet rejection for the indicated centrality bins. Fig. 3 shows the comparison of the corrected and measured R_{CP} values as a function of jet p_{T} for $R = 0.2$ and $R = 0.4$ jets in the 0–10% centrality bin. The unfolding has little effect on the $R = 0.2$ R_{CP} due to the good energy resolution (relative to larger radii) for $R = 0.2$ jets even in central collisions. For the $R = 0.4$ jets, R_{CP} is reduced by a factor of about two at the lowest p_{T} values included in the analysis and is only slightly modified at the highest p_{T} . Because the unfolding provides a non-local mapping of the input jet p_{T} spectrum onto the unfolded spectrum, the statistical uncertainties in the unfolded spectra have significant correlations between bins, and there is not a direct relationship between the statistical errors in the input spectrum and the unfolded spectrum. The regularization of the unfolding also suppresses statistical fluctuations in the unfolded spectrum, but the statistical uncertainties in the measured spectrum also contributes to the systematic uncertainties from the unfolding procedure.

8. Systematic uncertainties

Systematic uncertainties in the R_{CP} measurement can arise due to errors on the jet energy scale (JES), the jet energy resolution (JER), jet finding efficiency, the unfolding procedure, and the R_{coll} values. Uncertainties in jet E_{T} and p_{T} are assumed to be equal (i.e. $\delta p_{\text{T}} = \delta E_{\text{T}}$). Uncertainties in the JES and the JER influence the unfolding of the jet spectra. The resulting systematic uncertainties on the R_{CP} values ($\delta R_{\text{CP}}^{\text{sys}}$) were evaluated by producing new response matrices according to the procedures described below, generating unfolded spectra from these matrices, and calculating new R_{CP} values. The resulting changes in the R_{CP} values were taken to be estimates of $\delta R_{\text{CP}}^{\text{sys}}$. For uncertainties fully correlated in centrality, $\delta R_{\text{CP}}^{\text{sys}}$ was evaluated by simultaneously varying the chosen centrality bin and the 60–80% bin, while for other uncertainties, the chosen centrality bin and 60–80% centrality bins were varied separately and the variations in R_{CP} combined in quadrature.

Overall JES uncertainties common to the different centrality bins cancel in the ratio of the spectra in R_{CP} , but centrality-dependent JES errors will produce a systematic shift in R_{CP} . Studies using the MC overlay sample discussed in Section 6 indicate a maximum difference in JES between the 0–10% and 60–80% centrality bins for the jet p_{T} range included in this analysis of 0.5%, 1%, 1.5% and 2.5% for $R = 0.2, 0.3, 0.4$ and 0.5, respectively. Studies were also performed with the data overlay sample using an identical procedure as that applied to the MC overlay sample. The JES evaluated in the data overlay was found to agree between the 0–10% and 60–80% centrality bins to better than 1%, which is better than the agreement found in the MC overlay sample.

Independent evaluations of a possible centrality dependence of the calorimeter JES were performed by matching track and calorimeter jets in both the data and the MC overlay sample. The track jets provide a common reference for evaluating calorimeter jet response that is insensitive to the UE. The average calorimeter jet E_{T} was evaluated as a function of matching track jet p_{T} , $\langle E_{\text{T}}^{\text{calo}} \rangle(p_{\text{T}}^{\text{trkjet}})$, for different centrality bins. In the data, for $p_{\text{T}}^{\text{trkjet}} > 50$ GeV, the $\langle E_{\text{T}}^{\text{calo}} \rangle$ values were found to be consistent across all centrality bins to better than 3%. Accounting for a slight centrality dependence seen in the MC overlay sample, the 0–10% and 60–80% bins agree to 2%. For $p_{\text{T}}^{\text{trkjet}} < 50$ GeV, R - and centrality-dependent differences of up to 4% (for $R = 0.5$) are observed between data and MC overlay results for $\langle E_{\text{T}}^{\text{calo}} \rangle(p_{\text{T}}^{\text{trkjet}})$. This study provides a stringent constraint on changes in calorimeter response for jets af-

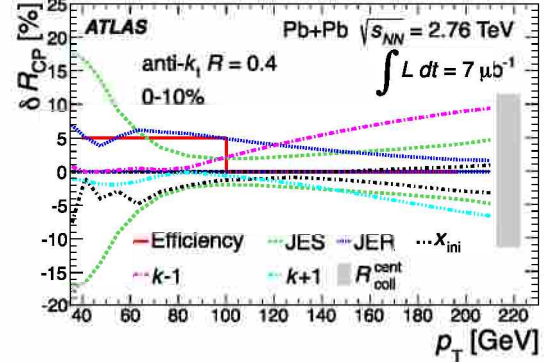


Fig. 4. Contributions to the relative systematic uncertainty on the R_{CP} from various sources for the $R = 0.4$ anti- k_{t} jets in the 0–10% centrality bin. The $k \pm 1$ curves denote the uncertainty due to the choice of regularization parameter obtained by unfolding with the fourth and sixth singular values. A constant 5% systematic uncertainty on the jet reconstruction efficiency is assigned for $p_{\text{T}} < 100$ GeV only. The 11% uncertainty in the determination of R_{coll} is indicated with a shaded box and is p_{T} -independent.

fected by quenching and justifies the use of unquenched jets from PYTHIA in evaluating the jet performance and response matrices.

Based on the combination of the studies described above, the systematic uncertainties on the centrality dependence of the JES for the 0–10% centrality bin and for calorimeter jet $p_{\text{T}} > 70$ GeV were estimated to be 0.5%, 1%, 1.5% and 2.5%, respectively, for $R = 0.2, 0.3, 0.4$ and 0.5 jets. At lower p_{T} , the assigned systematic uncertainties increase linearly with decreasing p_{T} such that they double in size between 70 GeV and 38 GeV. For other centrality bins, the systematic errors on the centrality dependence of the JES decrease smoothly from central to peripheral collisions. The resulting $\delta R_{\text{CP}}^{\text{sys}}$ values were evaluated using new response matrices generated by scaling the reconstructed p_{T} to account for the above-quoted JES uncertainties. The JES systematic uncertainty is assumed to be fully correlated between different centrality bins and different R values.

Systematic uncertainties in the JER due to inaccuracies in the MC description of the UE fluctuations were evaluated using results of the fluctuation analysis described above. The effects of those inaccuracies were evaluated by rescaling the per-jet $\Delta p_{\text{T}} \equiv p_{\text{T}}^{\text{rec}} - p_{\text{T}}^{\text{truth}}$ values obtained from the MC study by factors that cover the differences between data and MC result. For each centrality and jet radius, a modified value of the b parameter in Eq. (4) was evaluated and used to obtain new JER values, $\sigma'[\Delta E_{\text{T}}]$ from Eq. (4). Then a rescaled Δp_{T} was obtained from

$$\Delta p_{\text{T}}' = \Delta p_{\text{T}} \left(\frac{\sigma'}{\sigma} \right). \quad (7)$$

Since the discrepancies between the MC and the data were observed to be different for positive and negative fluctuations, the rescaling was applied separately for positive and negative Δp_{T} .

The ΣE_{T} values in the MC study were found to have larger positive fluctuations than those in the data for all centralities by approximately 2.5%, 2.5%, 5%, and 7.5% for $R = 0.2, 0.3, 0.4$ and 0.5 jets, respectively, so for positive Δp_{T} , b was reduced by these percentages. For the 0–10% centrality bin, the negative fluctuations were also larger in the MC study than in the data by the same approximate percentages, so for central collisions the same, modified b value was used for negative Δp_{T} . For all other centrality bins, the negative fluctuations in the data were larger than in the MC by approximately twice the above-quoted percentages. Thus, for those centralities, the modified b values were obtained for negative Δp_{T} by increasing b by 5%, 5%, 10%, and 15%, respectively, for $R = 0.2, 0.3, 0.4$ and 0.5 jets.

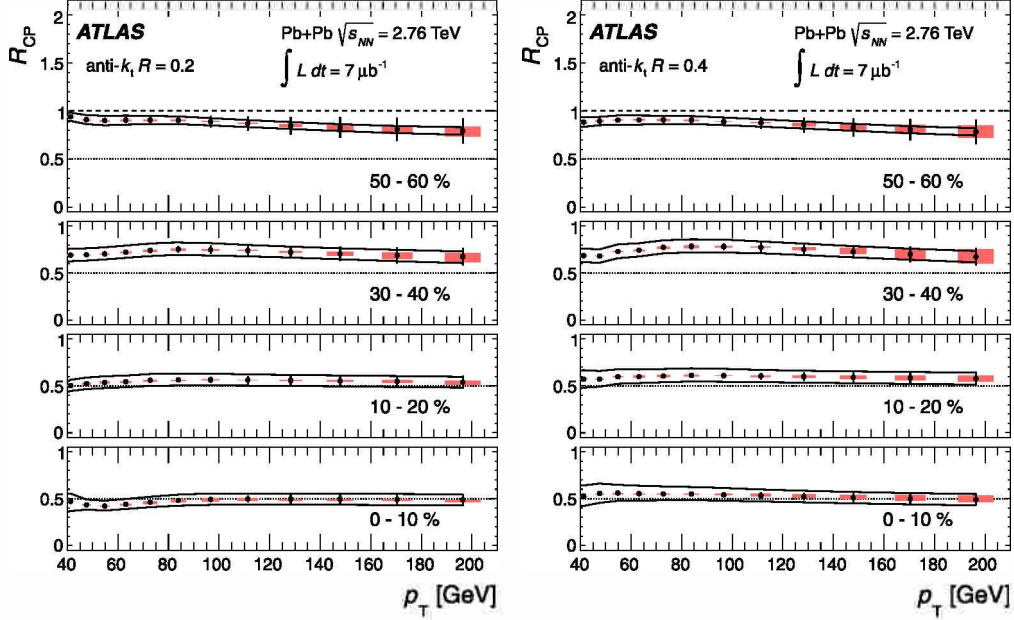


Fig. 5. R_{CP} values as a function of jet p_{T} for $R = 0.2$ (left) and $R = 0.4$ (right) anti- k_{T} jets in four bins of collision centrality. The error bars indicate statistical errors from the unfolding, the shaded boxes indicate unfolding regularization systematic errors that are partially correlated between points. The solid lines indicate systematic errors that are fully correlated between all points. The horizontal width of the systematic error band is chosen for presentation purposes only. Dotted lines indicate $R_{\text{CP}} = 1$.

New response matrices were generated using the calculated $\Delta p_{\text{T}}^{\text{rec}}$ values according to $p_{\text{T}}^{\text{rec}} = p_{\text{T}}^{\text{truth}} + \Delta p_{\text{T}}^{\text{rec}}$, and these modified response matrices were used to estimate the JER systematic uncertainties following the procedure described above. The systematic uncertainty on the spectra due to the JER for the 0–10% centrality bin was taken to be one-sided as all evaluations indicate that the MC simulations slightly overestimate UE fluctuations. Asymmetric errors were obtained for the other centrality bins by applying the positive and negative ΔE_{T} scalings separately. The JER systematic uncertainties were assumed to be fully correlated between different jet R values but uncorrelated between different collision centralities, so the uncertainties on the spectra were combined in quadrature in evaluating $\delta R_{\text{CP}}^{\text{sys}}$. The conservative assumption that the JER uncertainties are fully uncorrelated between different centrality bins is based on the observation that the differences between data and the HIJING MC sample in the fluctuation analysis are not the same for all centralities.

The systematic uncertainties associated with the non-UE contributions to the JER (described by the a and c terms in Eq. (4)) were evaluated following procedures used by ATLAS in previous pp jet measurements [41]. New response matrices were generated by applying an additional stochastic smearing to the Δp_{T} values, and the systematic uncertainty was obtained by applying the procedure described above.

Systematic uncertainties on R_{CP} due to the unfolding were evaluated by changing the power index (n) in the functional form for x_{ini} by ± 0.5 and by varying the regularization parameter. The ± 0.5 change in the power law index was chosen because it produces a spectrum that changes relative to the default x_{ini} over the measured p_{T} range by a factor of about two – the typical suppression observed in central collisions. Thus, it covers the possibility that the true R_{CP} could increase to one or decrease to 0.25 over the measured p_{T} range. To evaluate the potential systematic uncertainty due to regularization, the unfolding was performed with regularization parameters obtained from the fourth and sixth singular values of the unfolding matrix, $\tau = s_4^2$ and $\tau = s_6^2$. Systematic uncertainties on the spectra were determined from the differences

in the unfolded spectra. The resulting $\delta R_{\text{CP}}^{\text{sys}}$ values were obtained assuming that the regularization uncertainties on the two spectra are uncorrelated.

The systematic uncertainty on the efficiency correction was evaluated by comparing MC overlay and data overlay samples where differences less than 5% were observed on the “turn on” part of the efficiency curve. A 5% uncertainty due to the efficiency correction was applied to R_{CP} for $p_{\text{T}} < 100$ GeV in the four most central bins. To check for biases introduced by the UE jet rejection, the analysis was repeated with a significantly weakened rejection criterion in which jets were required to match a single track with $p_{\text{T}} > 4$ GeV. No significant differences in the R_{CP} were observed except for $p_{\text{T}} < 50$ GeV where differences as high as 4% were found. These differences can be attributed to the contribution of additional UE jets.

The different contributions to the total $\delta R_{\text{CP}}^{\text{sys}}$ are shown in Fig. 4 for $R = 0.4$ jets in the 0–10% centrality bin. The JES and x_{ini} uncertainties are approximately independent of p_{T} , while the JER uncertainty decreases with increasing p_{T} . The regularization uncertainty grows with increasing p_{T} due to the poorer statistical precision of the high- p_{T} points. The systematic uncertainties for the other radii show similar p_{T} and centrality dependence, with the JES and JER uncertainties increasing with jet radius as expected.

9. Results

Fig. 5 shows the R_{CP} values obtained for $R = 0.2$ and $R = 0.4$ jets as a function of p_{T} in four bins of collision centrality with three different error contributions: statistical uncertainties, partially correlated systematic uncertainties, and fully correlated uncertainties. The R_{CP} values for all centralities and for both jet radii are observed to have at most a weak variation with p_{T} . For the 0–10% centrality bin the R_{CP} values for both jet radii show a factor of about two suppression in the $1/N_{\text{coll}}$ -scaled jet yield. For more peripheral collisions, R_{CP} increases at all jet p_{T} relative to central collisions, with the R_{CP} values reaching 0.9 for the 50–60% centrality bin. A more detailed evaluation of the centrality dependence

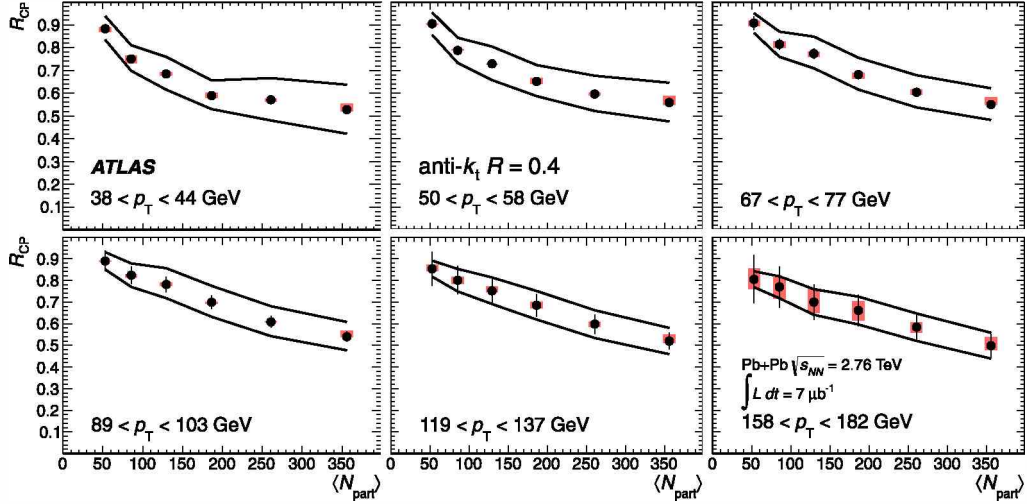


Fig. 6. R_{CP} values as a function of N_{part} for $R = 0.4$ anti- k_t jets in six p_T bins. The error bars indicate statistical errors from the unfolding; the shaded boxes indicate point-to-point systematic errors that are only partially correlated. The solid lines indicate systematic errors that are fully correlated between all points. The horizontal errors indicate systematic uncertainties on N_{part} .

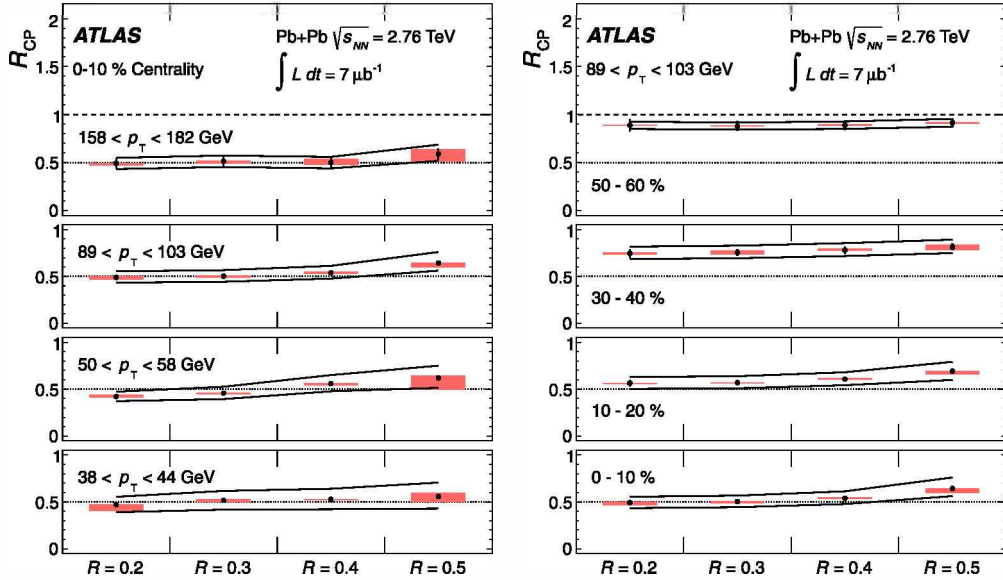


Fig. 7. Left: R_{CP} in the 0–10% centrality bin as a function of jet radius for four bins of jet p_T . Right: R_{CP} as a function of jet radius for four centrality bins for the p_T interval $89 < p_T < 103$ GeV. The error bars indicate statistical errors from the unfolding; the shaded boxes indicate point-to-point systematic errors that are only partially correlated. The solid lines indicate systematic errors that are fully correlated between all points. The horizontal width of the systematic error band is chosen for presentation purposes only. Dotted lines indicate $R_{CP} = 0.5$, and the dashed lines on the top panels indicate $R_{CP} = 1$.

of R_{CP} for $R = 0.4$ jets is presented in Fig. 6, which shows R_{CP} vs N_{part} for six jet p_T bins. R_{CP} decreases monotonically with increasing N_{part} for all p_T bins. The lower p_T bins, for which the data are more statistically precise, show a variation of R_{CP} with N_{part} that is most rapid at low N_{part} . Trends similar to those shown in Figs. 5 and 6 are observed for all jet radii.

The dependence of R_{CP} on jet radius is shown in Fig. 7 for the 0–10% centrality bin in four jet p_T intervals (left) and for different centrality bins in the $89 < p_T < 103$ GeV bin (right). For this figure, the shaded boxes indicate the combined contribution of systematic uncertainties due to regularization, x_{ini} , and efficiency, which are only partially correlated between points. All other systematic errors are fully correlated and are indicated by solid lines. The results in Fig. 7 show a weak variation of R_{CP} with R , that is nonetheless significant when taking into account the correlations in the errors between the different R values.

To demonstrate this conclusion more clearly, Fig. 8 shows the ratio of R_{CP} values between $R = 0.3, 0.4$ and 0.5 jets and $R = 0.2$ jets, $R_{CP}^R/R_{CP}^{0.2}$, as a function of p_T for the 0–10% centrality bin. When evaluating the ratio, there is significant cancellation between the correlated systematic uncertainties. Statistical correlations between the jet yields for the different radii were evaluated in the measured spectra and tracked through the unfolding procedure separately for the 0–10% and 60–80% centrality bins. Those correlations were then included when evaluating the statistical errors on $R_{CP}^R/R_{CP}^{0.2}$ shown in Fig. 8. The results in that figure indicate a significant dependence of R_{CP} on jet radius. For $p_T < 100$ GeV the $R_{CP}^R/R_{CP}^{0.2}$ values for both $R = 0.4$ and $R = 0.5$ differ from one beyond the statistical and systematic uncertainties. The deviation persists for $R = 0.5$ above 100 GeV. A similar, but weaker dependence is observed in the 10–20% centrality bin. In more peripheral bins, no significant radial dependence is observed. The differences

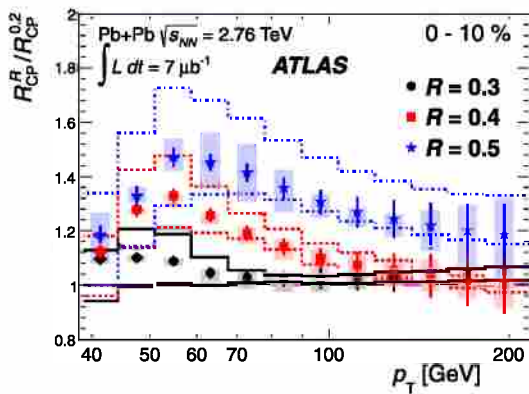


Fig. 8. Ratios of R_{CP} values between $R = 0.3, 0.4$ and 0.5 jets and $R = 0.2$ jets as a function of p_T in the $0\text{--}10\%$ centrality bin. The error bars show statistical uncertainties (see text). The shaded boxes indicate partially correlated systematic errors. The lines indicate systematic errors that are fully correlated between different p_T bins.

between R_{CP} values for the different jet radii increase with decreasing p_T , except for the lowest two p_T bins. However, direct comparisons of R_{CP} between different jet radii at low p_T should be treated with care as the same jets measured using smaller radii will tend to appear in lower p_T bins than when measured with a larger radius.

10. Conclusions

This Letter presents results of measurements of the centrality dependence of jet suppression, characterized by the inclusive jet central-to-peripheral ratio, R_{CP} , in $\text{Pb} + \text{Pb}$ collisions at 2.76 TeV per nucleon at the LHC. The measurements were performed over the p_T range $38 < p_T < 210$ GeV for anti- k_t jets of radii $R = 0.2, 0.3, 0.4$ and 0.5 . The inclusive jet yield is observed to be suppressed by a factor of about two in central collisions relative to peripheral collisions with at most a weak p_T dependence to the suppression. The suppression varies monotonically with collision centrality over the measured p_T range and for all jet radii. The R_{CP} at fixed p_T is observed to vary with jet radius increasing gradually from $R = 0.2$ to $R = 0.5$. That variation is most significant for $p_T < 100$ GeV where more than a 30% variation is observed. These results provide the first direct measurement of inclusive jet suppression in heavy ion collisions. The substantial suppression of the jet yield observed at all p_T values complements the previous measurements of dijet transverse energy imbalance in $\text{Pb} + \text{Pb}$ collisions at the LHC [13–15].

Acknowledgements

We thank CERN for the very successful operation of the LHC, as well as the support staff from our institutions without whom ATLAS could not be operated efficiently.

We acknowledge the support of ANPCyT, Argentina; YerPhI, Armenia; ARC, Australia; BMWF, Austria; ANAS, Azerbaijan; SSTC, Belarus; CNPq and FAPESP, Brazil; NSERC, NRC and CFI, Canada; CERN; CONICYT, Chile; CAS, MOST and NSFC, China; COLCIENCIAS, Colombia; MSMT CR, MPO CR and VSC CR, Czech Republic; DNRF, DNSRC and Lundbeck Foundation, Denmark; EPLANET and ERC, European Union; IN2P3-CNRS, CEA-DSM/IRFU, France; GNAS, Georgia; BMBF, DFG, HGF, MPG and AvH Foundation, Germany; GSRT, Greece ISF, MINERVA, GIF, DIP and Benoziyo Center, Israel; INFN, Italy; MEXT and JSPS, Japan; CNRST, Morocco; FOM and NWO, Netherlands; RCN, Norway; MNiSW, Poland; GRICES and FCT, Portugal; MERYS (MECTS), Romania; MES of Russia and ROSATOM, Russian Federation; JINR; MSTD, Serbia; MSSR, Slovakia; ARRS and

MVZT, Slovenia; DST/NRF, South Africa; MICINN, Spain; SRC and Wallenberg Foundation, Sweden; SER, SNSF and Cantons of Bern and Geneva, Switzerland; NSC, Taiwan; TAEK, Turkey; STFC, the Royal Society and Leverhulme Trust, United Kingdom; DOE and NSF, United States of America.

The crucial computing support from all WLCG partners is acknowledged gratefully, in particular from CERN and the ATLAS Tier-1 facilities at TRIUMF (Canada), NDGF (Denmark, Norway, Sweden), CC-IN2P3 (France), KIT/GridKA (Germany), INFN-CNAF (Italy), NL-T1 (Netherlands), PIC (Spain), ASGC (Taiwan), RAL (UK) and BNL (USA) and in the Tier-2 facilities worldwide.

Open access

This article is published Open Access at sciedirect.com. It is distributed under the terms of the Creative Commons Attribution License 3.0, which permits unrestricted use, distribution, and reproduction in any medium, provided the original authors and source are credited.

References

- [1] N. Armesto, et al., *J. Phys. G* 35 (2008) 054001, arXiv:0711.0974.
- [2] X.-N. Wang, M. Gyulassy, M. Plumer, *Phys. Rev. D* 51 (1995) 3436, arXiv:hep-ph/9408344.
- [3] R. Baier, Y.L. Dokshitzer, A.H. Mueller, D. Schiff, *Phys. Rev. C* 58 (1998) 1706, arXiv:hep-ph/9803473.
- [4] M. Gyulassy, P. Levai, I. Vitev, *Phys. Rev. Lett.* 85 (2000) 5535, arXiv:nucl-th/0005032.
- [5] S.S. Adler, et al., *Phys. Rev. Lett.* 91 (2003) 072301, arXiv:nucl-ex/0304022.
- [6] J. Adams, et al., *Phys. Rev. Lett.* 91 (2003) 172302, arXiv:nucl-ex/0305015.
- [7] I. Arsene, et al., *Phys. Rev. Lett.* 91 (2003) 072305, arXiv:nucl-ex/0307003.
- [8] B.B. Back, et al., *Phys. Rev. Lett.* 94 (2005) 082304, arXiv:nucl-ex/0405003.
- [9] C. Adler, et al., *Phys. Rev. Lett.* 90 (2003) 082302, arXiv:nucl-ex/0210033.
- [10] A. Adare, et al., *Phys. Rev. C* 78 (2008) 014901, arXiv:0801.4545.
- [11] K. Adcox, et al., *Nucl. Phys. A* 757 (2005) 184, arXiv:nucl-ex/0410003.
- [12] J. Adams, et al., *Nucl. Phys. A* 757 (2005) 102, arXiv:nucl-ex/0501009.
- [13] ATLAS Collaboration, *Phys. Rev. Lett.* 105 (2010) 252303, arXiv:1011.6182.
- [14] CMS Collaboration, *Phys. Rev. C* 84 (2011) 024906, arXiv:1102.1957.
- [15] CMS Collaboration, CERN-PH-EP-2012-042, 2012, arXiv:1202.5022.
- [16] J.D. Bjorken, Fermilab Preprint, FERMILAB-PUB-82-059-THY.
- [17] N. Armesto, B. Cole, C. Gale, W.A. Horowitz, P. Jacobs, et al., *Phys. Rev. C* 86 (2012) 064904, arXiv:1106.1106.
- [18] I. Vitev, S. Wicks, B.-W. Zhang, *JHEP* 0811 (2008) 093, arXiv:0810.2807.
- [19] I. Vitev, B.-W. Zhang, *Phys. Rev. Lett.* 104 (2010) 132001, arXiv:0910.1090.
- [20] Y. He, I. Vitev, B.-W. Zhang, arXiv:1105.2566.
- [21] G.-Y. Qin, B. Muller, *Phys. Rev. Lett.* 106 (2011) 162302, arXiv:1012.5280; G.-Y. Qin, B. Muller, *Phys. Rev. Lett.* 108 (2012) 189904 (Erratum).
- [22] M. Cacciari, G.P. Salam, G. Soyez, *JHEP* 0804 (2008) 063, arXiv:0802.1189.
- [23] ATLAS Collaboration, *JINST* 3 (2008) S08003.
- [24] ATLAS Collaboration, *Eur. Phys. J. C* 70 (2010) 787, arXiv:1004.5293.
- [25] T. Cornelissen, M. Elsing, I. Gavrilko, W. Liebig, E. Moyse, et al., *J. Phys. Conf. Ser.* 119 (2008) 032014.
- [26] ATLAS Collaboration, *Phys. Lett. B* 707 (2012) 330, arXiv:1108.6018.
- [27] O. Djupsland, J. Nystrand, *Phys. Rev. C* 83 (2010) 041901, arXiv:1011.4908.
- [28] B. Alver, M. Baker, C. Loizides, P. Steinberg, arXiv:0805.4411.
- [29] M.L. Miller, K. Reiglers, S.J. Sanders, P. Steinberg, *Ann. Rev. Nucl. Part. Sci.* 57 (2007) 205, arXiv:nucl-ex/0701025.
- [30] ATLAS Collaboration, *Eur. Phys. J. C* 70 (2010) 823, arXiv:1005.4568.
- [31] X.-N. Wang, M. Gyulassy, *Phys. Rev. D* 44 (1991) 3501.
- [32] M. Masera, G. Ortona, M. Poghosyan, F. Prino, *Phys. Rev. C* 79 (2009) 064909.
- [33] S. Agostinelli, et al., *Nucl. Instrum. Meth. A* 506 (2003) 250.
- [34] ATLAS Collaboration, *New J. Phys.* 13 (2010) 053033, arXiv:1012.5104.
- [35] T. Sjostrand, S. Mrenna, P.Z. Skands, *JHEP* 0605 (2006) 026, arXiv:hep-ph/0603175.
- [36] ATLAS Collaboration, *Eur. Phys. J. C*, in press, arXiv:1112.6426.
- [37] A.M. Poskanzer, S. Voloshin, *Phys. Rev. C* 58 (1998) 1671, arXiv:nucl-ex/9805001.
- [38] ATLAS Collaboration, CERN-OPEN-2008-20, arXiv:0901.0512.
- [39] A. Hocker, V. Kartvelishvili, *Nucl. Instrum. Meth. A* 372 (1996) 469, arXiv:hep-ph/9509307.
- [40] T. Adye, in: *Proceedings of the PHYSTAT 2009 Workshop*, CERN, Geneva, Switzerland, January 2011, CERN-2011-006, p. 313, arXiv:1105.1160.
- [41] ATLAS Collaboration, *Eur. Phys. J. C* 71 (2011) 1512, arXiv:1009.5908.

ATLAS Collaboration

- G. Aad⁴⁸, B. Abbott¹¹¹, J. Abdallah¹¹, S. Abdel Khalek¹¹⁵, A.A. Abdelalim⁴⁹, O. Abdinov¹⁰, B. Abi¹¹², M. Abolins⁸⁸, O.S. AbouZeid¹⁵⁸, H. Abramowicz¹⁵³, H. Abreu¹³⁶, E. Acerbi^{89a,89b}, B.S. Acharya^{164a,164b}, L. Adamczyk³⁷, D.L. Adams²⁴, T.N. Addy⁵⁶, J. Adelman¹⁷⁶, S. Adomeit⁹⁸, P. Adragna⁷⁵, T. Adye¹²⁹, S. Aefsky²², J.A. Aguilar-Saavedra^{124b,a}, M. Agustoni¹⁶, M. Aharrouche⁸¹, S.P. Ahlen²¹, F. Ahles⁴⁸, A. Ahmad¹⁴⁸, M. Ahsan⁴⁰, G. Aielli^{133a,133b}, T. Akdogan^{18a}, T.P.A. Åkesson⁷⁹, G. Akimoto¹⁵⁵, A.V. Akimov⁹⁴, M.S. Alam¹, M.A. Alam⁷⁶, J. Albert¹⁶⁹, S. Albrand⁵⁵, M. Aleksandrov⁶⁴, F. Alessandria^{89a}, C. Alexa^{25a}, G. Alexander¹⁵³, G. Alexandre⁴⁹, T. Alexopoulos⁹, M. Alhroob^{164a,164c}, M. Aliev¹⁵, G. Alimonti^{89a}, J. Alison¹²⁰, B.M.M. Allbrooke¹⁷, P.P. Allport⁷³, S.E. Allwood-Spiers⁵³, J. Almond⁸², A. Aloisio^{102a,102b}, R. Alon¹⁷², A. Alonso⁷⁹, B. Alvarez Gonzalez⁸⁸, M.G. Alviggi^{102a,102b}, K. Amako⁶⁵, C. Amelung²², V.V. Ammosov¹²⁸, A. Amorim^{124a,b}, N. Amram¹⁵³, C. Anastopoulos²⁹, L.S. Ancu¹⁶, N. Andari¹¹⁵, T. Andeen³⁴, C.F. Anders^{58b}, G. Anders^{58a}, K.J. Anderson³⁰, A. Andreazza^{89a,89b}, V. Andrei^{58a}, X.S. Anduaga⁷⁰, P. Anger⁴³, A. Angerami³⁴, F. Anghinolfi²⁹, A. Anisenkov¹⁰⁷, N. Anjos^{124a}, A. Annovi⁴⁷, A. Antonaki⁸, M. Antonelli⁴⁷, A. Antonov⁹⁶, J. Antos^{144b}, F. Anulli^{132a}, S. Aoun⁸³, L. Aperio Bella⁴, R. Apolle^{118,c}, G. Arabidze⁸⁸, I. Aracena¹⁴³, Y. Arai⁶⁵, A.T.H. Arce⁴⁴, S. Arfaoui¹⁴⁸, J.-F. Arguin¹⁴, E. Arik^{18a,*}, M. Arik^{18a}, A.J. Armbruster⁸⁷, O. Arnaez⁸¹, V. Arnal⁸⁰, C. Arnault¹¹⁵, A. Artamonov⁹⁵, G. Artoni^{132a,132b}, D. Arutinov²⁰, S. Asai¹⁵⁵, R. Asfandiyarov¹⁷³, S. Ask²⁷, B. Åsman^{146a,146b}, L. Asquith⁵, K. Assamagan²⁴, A. Astbury¹⁶⁹, B. Aubert⁴, E. Auge¹¹⁵, K. Augsten¹²⁷, M. Aurousseau^{145a}, G. Avolio¹⁶³, R. Avramidou⁹, D. Axen¹⁶⁸, G. Azuelos^{93,d}, Y. Azuma¹⁵⁵, M.A. Baak²⁹, G. Baccaglioni^{89a}, C. Bacci^{134a,134b}, A.M. Bach¹⁴, H. Bachacou¹³⁶, K. Bachas²⁹, M. Backes⁴⁹, M. Backhaus²⁰, E. Badescu^{25a}, P. Bagnaia^{132a,132b}, S. Bahinipati², Y. Bai^{32a}, D.C. Bailey¹⁵⁸, T. Bain¹⁵⁸, J.T. Baines¹²⁹, O.K. Baker¹⁷⁶, M.D. Baker²⁴, S. Baker⁷⁷, E. Banas³⁸, P. Banerjee⁹³, Sw. Banerjee¹⁷³, D. Banfi²⁹, A. Bangert¹⁵⁰, V. Bansal¹⁶⁹, H.S. Bansil¹⁷, L. Barak¹⁷², S.P. Baranov⁹⁴, A. Barbaro Galtieri¹⁴, T. Barber⁴⁸, E.L. Barberio⁸⁶, D. Barberis^{50a,50b}, M. Barbero²⁰, D.Y. Bardin⁶⁴, T. Barillari⁹⁹, M. Barisonzi¹⁷⁵, T. Barklow¹⁴³, N. Barlow²⁷, B.M. Barnett¹²⁹, R.M. Barnett¹⁴, A. Baroncelli^{134a}, G. Barone⁴⁹, A.J. Barr¹¹⁸, F. Barreiro⁸⁰, J. Barreiro Guimarães da Costa⁵⁷, P. Barrillon¹¹⁵, R. Bartoldus¹⁴³, A.E. Barton⁷¹, V. Bartsch¹⁴⁹, R.L. Bates⁵³, L. Batkova^{144a}, J.R. Batley²⁷, A. Battaglia¹⁶, M. Battistin²⁹, F. Bauer¹³⁶, H.S. Bawa^{143,e}, S. Beale⁹⁸, T. Beau⁷⁸, P.H. Beauchemin¹⁶¹, R. Beccherle^{50a}, P. Bechtle²⁰, H.P. Beck¹⁶, A.K. Becker¹⁷⁵, S. Becker⁹⁸, M. Beckingham¹³⁸, K.H. Becks¹⁷⁵, A.J. Beddall^{18c}, A. Beddall^{18c}, S. Bedikian¹⁷⁶, V.A. Bednyakov⁶⁴, C.P. Bee⁸³, M. Begel²⁴, S. Behar Harpaz¹⁵², M. Beimforde⁹⁹, C. Belanger-Champagne⁸⁵, P.J. Bell⁴⁹, W.H. Bell⁴⁹, G. Bella¹⁵³, L. Bellagamba^{19a}, F. Bellina²⁹, M. Bellomo²⁹, A. Belloni⁵⁷, O. Beloborodova^{107,f}, K. Belotskiy⁹⁶, O. Beltramello²⁹, O. Benary¹⁵³, D. Benchekroun^{135a}, K. Bendtz^{146a,146b}, N. Benekos¹⁶⁵, Y. Benhammou¹⁵³, E. Benhar Noccioli⁴⁹, J.A. Benitez Garcia^{159b}, D.P. Benjamin⁴⁴, M. Benoit¹¹⁵, J.R. Bensinger²², K. Benslama¹³⁰, S. Bentvelsen¹⁰⁵, D. Berge²⁹, E. Bergeaas Kuutmann⁴¹, N. Berger⁴, F. Berghausen¹⁶⁹, E. Berglund¹⁰⁵, J. Beringer¹⁴, P. Bernat⁷⁷, R. Bernhard⁴⁸, C. Bernius²⁴, T. Berry⁷⁶, C. Bertella⁸³, A. Bertin^{19a,19b}, F. Bertolucci^{122a,122b}, M.I. Besana^{89a,89b}, G.J. Besjes¹⁰⁴, N. Besson¹³⁶, S. Bethke⁹⁹, W. Bhimji⁴⁵, R.M. Bianchi²⁹, M. Bianco^{72a,72b}, O. Biebel⁹⁸, S.P. Bieniek⁷⁷, K. Bierwagen⁵⁴, J. Biesiada¹⁴, M. Biglietti^{134a}, H. Bilokon⁴⁷, M. Bindi^{19a,19b}, S. Binet¹¹⁵, A. Bingul^{18c}, C. Bini^{132a,132b}, C. Biscarat¹⁷⁸, U. Bitenc⁴⁸, K.M. Black²¹, R.E. Blair⁵, J.-B. Blanchard¹³⁶, G. Blanchot²⁹, T. Blazek^{144a}, C. Blocker²², J. Blocki³⁸, A. Blondel⁴⁹, W. Blum⁸¹, U. Blumenschein⁵⁴, G.J. Bobbink¹⁰⁵, V.B. Bobrovnikov¹⁰⁷, S.S. Bocchetta⁷⁹, A. Bocci⁴⁴, C.R. Boddy¹¹⁸, M. Boehler⁴¹, J. Boek¹⁷⁵, N. Boelaert³⁵, J.A. Bogaerts²⁹, A. Bogdanchikov¹⁰⁷, A. Bogouch^{90,*}, C. Bohm^{146a}, J. Bohm¹²⁵, V. Boisvert⁷⁶, T. Bold³⁷, V. Boldea^{25a}, N.M. Bolnet¹³⁶, M. Bomben⁷⁸, M. Bona⁷⁵, M. Boonekamp¹³⁶, C.N. Booth¹³⁹, S. Bordoni⁷⁸, C. Borer¹⁶, A. Borisov¹²⁸, G. Borissov⁷¹, I. Borjanovic^{12a}, M. Borri⁸², S. Borroni⁸⁷, V. Bortolotto^{134a,134b}, K. Bos¹⁰⁵, D. Boscherini^{19a}, M. Bosman¹¹, H. Boterenbrood¹⁰⁵, D. Botterill¹²⁹, J. Bouchami⁹³, J. Boudreau¹²³, E.V. Bouhouva-Thacker⁷¹, D. Boumediene³³, C. Bourdarios¹¹⁵, N. Bousson⁸³, A. Boveia³⁰, J. Boyd²⁹, I.R. Boyko⁶⁴, I. Bozovic-Jelisavcic^{12b}, J. Bracinik¹⁷, P. Branchini^{134a}, A. Brandt⁷, G. Brandt¹¹⁸, O. Brandt⁵⁴, U. Bratzler¹⁵⁶, B. Brau⁸⁴, J.E. Brau¹¹⁴, H.M. Braun¹⁷⁵, S.F. Brazzale^{164a,164c}, B. Brelier¹⁵⁸, J. Bremer²⁹, K. Brendlinger¹²⁰, R. Brenner¹⁶⁶, S. Bressler¹⁷², D. Britton⁵³, F.M. Brochu²⁷, I. Brock²⁰, R. Brock⁸⁸, E. Brodet¹⁵³, F. Broggi^{89a}, C. Bromberg⁸⁸, J. Bronner⁹⁹, G. Brooijmans³⁴, T. Brooks⁷⁶,

- W.K. Brooks ^{31b}, G. Brown ⁸², H. Brown ⁷, P.A. Bruckman de Renstrom ³⁸, D. Bruncko ^{144b}, R. Bruneliere ⁴⁸, S. Brunet ⁶⁰, A. Bruni ^{19a}, G. Bruni ^{19a}, M. Bruschi ^{19a}, T. Buanes ¹³, Q. Buat ⁵⁵, F. Bucci ⁴⁹, J. Buchanan ¹¹⁸, P. Buchholz ¹⁴¹, R.M. Buckingham ¹¹⁸, A.G. Buckley ⁴⁵, S.I. Buda ^{25a}, I.A. Budagov ⁶⁴, B. Budick ¹⁰⁸, V. Büscher ⁸¹, L. Bugge ¹¹⁷, O. Bulekov ⁹⁶, A.C. Bundock ⁷³, M. Bunse ⁴², T. Buran ¹¹⁷, H. Burckhart ²⁹, S. Burdin ⁷³, T. Burgess ¹³, S. Burke ¹²⁹, E. Busato ³³, P. Bussey ⁵³, C.P. Buszello ¹⁶⁶, B. Butler ¹⁴³, J.M. Butler ²¹, C.M. Buttar ⁵³, J.M. Butterworth ⁷⁷, W. Buttlinger ²⁷, S. Cabrera Urbán ¹⁶⁷, D. Caforio ^{19a,19b}, O. Cakir ^{3a}, P. Calafiura ¹⁴, G. Calderini ⁷⁸, P. Calfayan ⁹⁸, R. Calkins ¹⁰⁶, L.P. Caloba ^{23a}, R. Caloi ^{132a,132b}, D. Calvet ³³, S. Calvet ³³, R. Camacho Toro ³³, P. Camarri ^{133a,133b}, D. Cameron ¹¹⁷, L.M. Caminada ¹⁴, S. Campana ²⁹, M. Campanelli ⁷⁷, V. Canale ^{102a,102b}, F. Canelli ^{30,g}, A. Canepa ^{159a}, J. Cantero ⁸⁰, R. Cantrill ⁷⁶, L. Capasso ^{102a,102b}, M.D.M. Capeans Garrido ²⁹, I. Caprini ^{25a}, M. Caprini ^{25a}, D. Capriotti ⁹⁹, M. Capua ^{36a,36b}, R. Caputo ⁸¹, R. Cardarelli ^{133a}, T. Carli ²⁹, G. Carlino ^{102a}, L. Carminati ^{89a,89b}, B. Caron ⁸⁵, S. Caron ¹⁰⁴, E. Carquin ^{31b}, G.D. Carrillo Montoya ¹⁷³, A.A. Carter ⁷⁵, J.R. Carter ²⁷, J. Carvalho ^{124a,h}, D. Casadei ¹⁰⁸, M.P. Casado ¹¹, M. Cascella ^{122a,122b}, C. Caso ^{50a,50b,*}, A.M. Castaneda Hernandez ^{173,i}, E. Castaneda-Miranda ¹⁷³, V. Castillo Gimenez ¹⁶⁷, N.F. Castro ^{124a}, G. Cataldi ^{72a}, P. Catastini ⁵⁷, A. Catinaccio ²⁹, J.R. Catmore ²⁹, A. Cattai ²⁹, G. Cattani ^{133a,133b}, S. Caughron ⁸⁸, P. Cavalleri ⁷⁸, D. Cavalli ^{89a}, M. Cavalli-Sforza ¹¹, V. Cavasinni ^{122a,122b}, F. Ceradini ^{134a,134b}, A.S. Cerqueira ^{23b}, A. Cerri ²⁹, L. Cerrito ⁷⁵, F. Cerutti ⁴⁷, S.A. Cetin ^{18b}, A. Chafaq ^{135a}, D. Chakraborty ¹⁰⁶, I. Chalupkova ¹²⁶, K. Chan ², B. Chapleau ⁸⁵, J.D. Chapman ²⁷, J.W. Chapman ⁸⁷, E. Chareyre ⁷⁸, D.G. Charlton ¹⁷, V. Chavda ⁸², C.A. Chavez Barajas ²⁹, S. Cheatham ⁸⁵, S. Chekanov ⁵, S.V. Chekulaev ^{159a}, G.A. Chelkov ⁶⁴, M.A. Chelstowska ¹⁰⁴, C. Chen ⁶³, H. Chen ²⁴, S. Chen ^{32c}, X. Chen ¹⁷³, Y. Chen ³⁴, A. Cheplakov ⁶⁴, R. Cherkaoui El Moursli ^{135e}, V. Chernyatin ²⁴, E. Cheu ⁶, S.L. Cheung ¹⁵⁸, L. Chevalier ¹³⁶, G. Chieffari ^{102a,102b}, L. Chikovani ^{51a}, J.T. Childers ²⁹, A. Chilingarov ⁷¹, G. Chiodini ^{72a}, A.S. Chisholm ¹⁷, R.T. Chislett ⁷⁷, A. Chitan ^{25a}, M.V. Chizhov ⁶⁴, G. Choudalakis ³⁰, S. Chouridou ¹³⁷, I.A. Christidi ⁷⁷, A. Christov ⁴⁸, D. Chromek-Burckhart ²⁹, M.L. Chu ¹⁵¹, J. Chudoba ¹²⁵, G. Ciapetti ^{132a,132b}, A.K. Ciftci ^{3a}, R. Ciftci ^{3a}, D. Cinca ³³, V. Cindro ⁷⁴, C. Ciocca ^{19a,19b}, A. Ciocio ¹⁴, M. Cirilli ⁸⁷, P. Cirkovic ^{12b}, M. Citterio ^{89a}, M. Ciubancan ^{25a}, A. Clark ⁴⁹, P.J. Clark ⁴⁵, R.N. Clarke ¹⁴, W. Cleland ¹²³, J.C. Clemens ⁸³, B. Clement ⁵⁵, C. Clement ^{146a,146b}, Y. Coadou ⁸³, M. Cobal ^{164a,164c}, A. Coccaro ¹³⁸, J. Cochran ⁶³, J.G. Cogan ¹⁴³, J. Coggeshall ¹⁶⁵, E. Cogneras ¹⁷⁸, J. Colas ⁴, A.P. Colijn ¹⁰⁵, N.J. Collins ¹⁷, C. Collins-Tooth ⁵³, J. Collot ⁵⁵, T. Colombo ^{119a,119b}, G. Colon ⁸⁴, P. Conde Muiño ^{124a}, E. Coniavitis ¹¹⁸, M.C. Conidi ¹¹, S.M. Consonni ^{89a,89b}, V. Consorti ⁴⁸, S. Constantinescu ^{25a}, C. Conta ^{119a,119b}, G. Conti ⁵⁷, F. Conventi ^{102a,j}, M. Cooke ¹⁴, B.D. Cooper ⁷⁷, A.M. Cooper-Sarkar ¹¹⁸, K. Copic ¹⁴, T. Cornelissen ¹⁷⁵, M. Corradi ^{19a}, F. Corriveau ^{85,k}, A. Cortes-Gonzalez ¹⁶⁵, G. Cortiana ⁹⁹, G. Costa ^{89a}, M.J. Costa ¹⁶⁷, D. Costanzo ¹³⁹, T. Costin ³⁰, D. Côté ²⁹, L. Courneyea ¹⁶⁹, G. Cowan ⁷⁶, C. Cowden ²⁷, B.E. Cox ⁸², K. Cranmer ¹⁰⁸, F. Crescioli ^{122a,122b}, M. Cristinziani ²⁰, G. Crosetti ^{36a,36b}, R. Crupi ^{72a,72b}, S. Crépé-Renaudin ⁵⁵, C.-M. Cuciuc ^{25a}, C. Cuénca Almenar ¹⁷⁶, T. Cuhadar Donszelmann ¹³⁹, M. Curatolo ⁴⁷, C.J. Curtis ¹⁷, C. Cuthbert ¹⁵⁰, P. Cwetanski ⁶⁰, H. Czirr ¹⁴¹, P. Czodrowski ⁴³, Z. Czyczula ¹⁷⁶, S. D'Auria ⁵³, M. D'Onofrio ⁷³, A. D'Orazio ^{132a,132b}, M.J. Da Cunha Sargedas De Sousa ^{124a}, C. Da Via ⁸², W. Dabrowski ³⁷, A. Dafinca ¹¹⁸, T. Dai ⁸⁷, C. Dallapiccola ⁸⁴, M. Dam ³⁵, M. Dameri ^{50a,50b}, D.S. Damiani ¹³⁷, H.O. Danielsson ²⁹, V. Dao ⁴⁹, G. Darbo ^{50a}, G.L. Darlea ^{25b}, W. Davey ²⁰, T. Davidek ¹²⁶, N. Davidson ⁸⁶, R. Davidson ⁷¹, E. Davies ^{118,c}, M. Davies ⁹³, A.R. Davison ⁷⁷, Y. Davygora ^{58a}, E. Dawe ¹⁴², I. Dawson ¹³⁹, R.K. Daya-Ishmukhametova ²², K. De ⁷, R. de Asmundis ^{102a}, S. De Castro ^{19a,19b}, S. De Cecco ⁷⁸, J. de Graat ⁹⁸, N. De Groot ¹⁰⁴, P. de Jong ¹⁰⁵, C. De La Taille ¹¹⁵, H. De la Torre ⁸⁰, F. De Lorenzi ⁶³, L. de Mora ⁷¹, L. De Nooij ¹⁰⁵, D. De Pedis ^{132a}, A. De Salvo ^{132a}, U. De Sanctis ^{164a,164c}, A. De Santo ¹⁴⁹, J.B. De Vivie De Regie ¹¹⁵, G. De Zorzi ^{132a,132b}, W.J. Dearnaley ⁷¹, R. Debbe ²⁴, C. Debenedetti ⁴⁵, B. Dechenaux ⁵⁵, D.V. Dedovich ⁶⁴, J. Degenhardt ¹²⁰, C. Del Papa ^{164a,164c}, J. Del Peso ⁸⁰, T. Del Prete ^{122a,122b}, T. Delemontex ⁵⁵, M. Deliyergiyev ⁷⁴, A. Dell'Acqua ²⁹, L. Dell'Asta ²¹, M. Della Pietra ^{102a,j}, D. della Volpe ^{102a,102b}, M. Delmastro ⁴, P.A. Delsart ⁵⁵, C. Deluca ¹⁰⁵, S. Demers ¹⁷⁶, M. Demichev ⁶⁴, B. Demirkoz ^{11,l}, J. Deng ¹⁶³, S.P. Denisov ¹²⁸, D. Derendarz ³⁸, J.E. Derkaoui ^{135d}, F. Derue ⁷⁸, P. Dervan ⁷³, K. Desch ²⁰, E. Devetak ¹⁴⁸, P.O. Deviveiros ¹⁰⁵, A. Dewhurst ¹²⁹, B. DeWilde ¹⁴⁸, S. Dhaliwal ¹⁵⁸, R. Dhullipudi ^{24,m}, A. Di Ciaccio ^{133a,133b}, L. Di Ciaccio ⁴, A. Di Girolamo ²⁹, B. Di Girolamo ²⁹, S. Di Luise ^{134a,134b}, A. Di Mattia ¹⁷³, B. Di Micco ²⁹, R. Di Nardo ⁴⁷, A. Di Simone ^{133a,133b}, R. Di Sipio ^{19a,19b}, M.A. Diaz ^{31a}, E.B. Diehl ⁸⁷, J. Dietrich ⁴¹, T.A. Dietzscht ^{58a},

- S. Diglio 86, K. Dindar Yagci 39, J. Dingfelder 20, F. Dinut 25a, C. Dionisi 132a, 132b, P. Dita 25a, S. Dita 25a,
 F. Dittus 29, F. Djama 83, T. Djorava 51b, M.A.B. do Vale 23c, A. Do Valle Wemans 124a,n, T.K.O. Doan 4,
 M. Dobbs 85, R. Dobinson 29,* D. Dobos 29, E. Dobson 29,o, J. Dodd 34, C. Doglioni 49, T. Doherty 53,
 Y. Doi 65,* J. Dolejsi 126, I. Dolenc 74, Z. Dolezal 126, B.A. Dolgoshein 96,* T. Dohmae 155, M. Donadelli 23d,
 J. Donini 33, J. Dopke 29, A. Doria 102a, A. Dos Anjos 173, A. Dotti 122a, 122b, M.T. Dova 70, A.D. Doxiadis 105,
 A.T. Doyle 53, M. Dris 9, J. Dubbert 99, S. Dube 14, E. Duchovni 172, G. Duckeck 98, A. Dudarev 29,
 F. Dudziak 63, M. Dührssen 29, I.P. Duerdorff 82, L. Duflot 115, M.-A. Dufour 85, M. Dunford 29,
 H. Duran Yildiz 3a, R. Duxfield 139, M. Dwuznik 37, F. Dydak 29, M. Düren 52, J. Ebke 98, S. Eckweiler 81,
 K. Edmonds 81, C.A. Edwards 76, N.C. Edwards 53, W. Ehrenfeld 41, T. Eifert 143, G. Eigen 13, K. Einsweiler 14,
 E. Eisenhandler 75, T. Ekelof 166, M. El Kacimi 135c, M. Ellert 166, S. Elles 4, F. Ellinghaus 81, K. Ellis 75,
 N. Ellis 29, J. Elmsheuser 98, M. Elsing 29, D. Emeliyanov 129, R. Engelmann 148, A. Engl 98, B. Epp 61,
 A. Eppig 87, J. Erdmann 54, A. Ereditato 16, D. Eriksson 146a, J. Ernst 1, M. Ernst 24, J. Ernwein 136,
 D. Errede 165, S. Errede 165, E. Ertel 81, M. Escalier 115, H. Esch 42, C. Escobar 123, X. Espinal Curull 11,
 B. Esposito 47, F. Etienne 83, A.I. Etiennevre 136, E. Etzion 153, D. Evangelakou 54, H. Evans 60, L. Fabbri 19a, 19b,
 C. Fabre 29, R.M. Fakhruddinov 128, S. Falciano 132a, Y. Fang 173, M. Fanti 89a, 89b, A. Farbin 7, A. Farilla 134a,
 J. Farley 148, T. Farooque 158, S. Farrell 163, S.M. Farrington 118, P. Farthouat 29, P. Fassnacht 29,
 D. Fassouliotis 8, B. Fatholahzadeh 158, A. Favareto 89a, 89b, L. Fayard 115, S. Fazio 36a, 36b, R. Febbraro 33,
 P. Federic 144a, O.L. Fedin 121, W. Fedorko 88, M. Fehling-Kaschek 48, L. Feligioni 83, D. Fellmann 5,
 C. Feng 32d, E.J. Feng 5, A.B. Fenyuk 128, J. Ferencei 144b, W. Fernando 5, S. Ferrag 53, J. Ferrando 53,
 V. Ferrara 41, A. Ferrari 166, P. Ferrari 105, R. Ferrari 119a, D.E. Ferreira de Lima 53, A. Ferrer 167,
 D. Ferrere 49, C. Ferretti 87, A. Ferretto Parodi 50a, 50b, M. Fiascaris 30, F. Fiedler 81, A. Filipčič 74,
 F. Filthaut 104, M. Fincke-Keeler 169, M.C.N. Fiolhais 124a,h, L. Fiorini 167, A. Firat 39, G. Fischer 41,
 M.J. Fisher 109, M. Flechl 48, I. Fleck 141, J. Fleckner 81, P. Fleischmann 174, S. Fleischmann 175, T. Flick 175,
 A. Floderus 79, L.R. Flores Castillo 173, M.J. Flowerdew 99, T. Fonseca Martin 16, A. Formica 136, A. Forti 82,
 D. Fortin 159a, D. Fournier 115, H. Fox 71, P. Francavilla 11, S. Franchino 119a, 119b, D. Francis 29, T. Frank 172,
 S. Franz 29, M. Fraternali 119a, 119b, S. Fratina 120, S.T. French 27, C. Friedrich 41, F. Friedrich 43, R. Froeschl 29,
 D. Froidevaux 29, J.A. Frost 27, C. Fukunaga 156, E. Fullana Torregrosa 29, B.G. Fulsom 143, J. Fuster 167,
 C. Gabaldon 29, O. Gabizon 172, T. Gadfort 24, S. Gadomski 49, G. Gagliardi 50a, 50b, P. Gagnon 60, C. Galea 98,
 E.J. Gallas 118, V. Gallo 16, B.J. Gallop 129, P. Gallus 125, K.K. Gan 109, Y.S. Gao 143,e, A. Gaponenko 14,
 F. Garberson 176, M. Garcia-Sciveres 14, C. García 167, J.E. García Navarro 167, R.W. Gardner 30, N. Garelli 29,
 H. Garitaonandia 105, V. Garonne 29, J. Garvey 17, C. Gatti 47, G. Gaudio 119a, B. Gaur 141, L. Gauthier 136,
 P. Gauzzi 132a, 132b, I.L. Gavrilenko 94, C. Gay 168, G. Gaycken 20, E.N. Gazis 9, P. Ge 32d, Z. Gecse 168,
 C.N.P. Gee 129, D.A.A. Geerts 105, Ch. Geich-Gimbel 20, K. Gellerstedt 146a, 146b, C. Gemme 50a,
 A. Gemmell 53, M.H. Genest 55, S. Gentile 132a, 132b, M. George 54, S. George 76, P. Gerlach 175,
 A. Gershon 153, C. Geweniger 58a, H. Ghazlane 135b, N. Ghodbane 33, B. Giacobbe 19a, S. Giagu 132a, 132b,
 V. Giakoumopoulou 8, V. Giangiobbe 11, F. Gianotti 29, B. Gibbard 24, A. Gibson 158, S.M. Gibson 29,
 D. Gillberg 28, A.R. Gillman 129, D.M. Gingrich 2,d, J. Ginzburg 153, N. Giokaris 8, M.P. Giordani 164c,
 R. Giordano 102a, 102b, F.M. Giorgi 15, P. Giovannini 99, P.F. Giraud 136, D. Giugni 89a, M. Giunta 93,
 P. Giusti 19a, B.K. Gjelsten 117, L.K. Gladilin 97, C. Glasman 80, J. Glatzer 48, A. Glazov 41, K.W. Glitza 175,
 G.L. Glonti 64, J.R. Goddard 75, J. Godfrey 142, J. Godlewski 29, M. Goebel 41, T. Göpfert 43, C. Goeringer 81,
 C. Gössling 42, S. Goldfarb 87, T. Golling 176, A. Gomes 124a,b, L.S. Gomez Fajardo 41, R. Gonçalo 76,
 J. Goncalves Pinto Firmino Da Costa 41, L. Gonella 20, S. Gonzalez 173, S. González de la Hoz 167,
 G. Gonzalez Parra 11, M.L. Gonzalez Silva 26, S. Gonzalez-Sevilla 49, J.J. Goodson 148, L. Goossens 29,
 P.A. Gorbounov 95, H.A. Gordon 24, I. Gorelov 103, G. Gorfine 175, B. Gorini 29, E. Gorini 72a, 72b,
 A. Gorišek 74, E. Gornicki 38, B. Gosdzik 41, A.T. Goshaw 5, M. Gosselink 105, M.I. Gostkin 64,
 I. Gough Eschrich 163, M. Gouighri 135a, D. Goujdami 135c, M.P. Goulette 49, A.G. Goussiou 138, C. Goy 4,
 S. Gozpınar 22, I. Grabowska-Bold 37, P. Grafström 19a, 19b, K.-J. Grahn 41, F. Grancagnolo 72a,
 S. Grancagnolo 15, V. Grassi 148, V. Gratchev 121, N. Grau 34, H.M. Gray 29, J.A. Gray 148, E. Graziani 134a,
 O.G. Grebenyuk 121, T. Greenshaw 73, Z.D. Greenwood 24,m, K. Gregersen 35, I.M. Gregor 41, P. Grenier 143,
 J. Griffiths 138, N. Grigalashvili 64, A.A. Grillo 137, S. Grinstein 11, Y.V. Grishkevich 97, J.-F. Grivaz 115,
 E. Gross 172, J. Grosse-Knetter 54, J. Groth-Jensen 172, K. Grybel 141, D. Guest 176, C. Guicheney 33,
 A. Guida 72a, 72b, S. Guindon 54, U. Gul 53, H. Guler 85,p, J. Gunther 125, B. Guo 158, J. Guo 34, P. Gutierrez 111,

- N. Guttman ¹⁵³, O. Gutzwiller ¹⁷³, C. Guyot ¹³⁶, C. Gwenlan ¹¹⁸, C.B. Gwilliam ⁷³, A. Haas ¹⁴³, S. Haas ²⁹, C. Haber ¹⁴, H.K. Hadavand ³⁹, D.R. Hadley ¹⁷, P. Haefner ²⁰, F. Hahn ²⁹, S. Haider ²⁹, Z. Hajduk ³⁸, H. Hakobyan ¹⁷⁷, D. Hall ¹¹⁸, J. Haller ⁵⁴, K. Hamacher ¹⁷⁵, P. Hamal ¹¹³, M. Hamer ⁵⁴, A. Hamilton ^{145b,q}, S. Hamilton ¹⁶¹, L. Han ^{32b}, K. Hanagaki ¹¹⁶, K. Hanawa ¹⁶⁰, M. Hance ¹⁴, C. Handel ⁸¹, P. Hanke ^{58a}, J.R. Hansen ³⁵, J.B. Hansen ³⁵, J.D. Hansen ³⁵, P.H. Hansen ³⁵, P. Hansson ¹⁴³, K. Hara ¹⁶⁰, G.A. Hare ¹³⁷, T. Harenberg ¹⁷⁵, S. Harkusha ⁹⁰, D. Harper ⁸⁷, R.D. Harrington ⁴⁵, O.M. Harris ¹³⁸, J. Hartert ⁴⁸, F. Hartjes ¹⁰⁵, T. Haruyama ⁶⁵, A. Harvey ⁵⁶, S. Hasegawa ¹⁰¹, Y. Hasegawa ¹⁴⁰, S. Hassani ¹³⁶, S. Haug ¹⁶, M. Hauschild ²⁹, R. Hauser ⁸⁸, M. Havranek ²⁰, C.M. Hawkes ¹⁷, R.J. Hawkings ²⁹, A.D. Hawkins ⁷⁹, D. Hawkins ¹⁶³, T. Hayakawa ⁶⁶, T. Hayashi ¹⁶⁰, D. Hayden ⁷⁶, C.P. Hays ¹¹⁸, H.S. Hayward ⁷³, S.J. Haywood ¹²⁹, M. He ^{32d}, S.J. Head ¹⁷, V. Hedberg ⁷⁹, L. Heelan ⁷, S. Heim ⁸⁸, B. Heinemann ¹⁴, S. Heisterkamp ³⁵, L. Helary ²¹, C. Heller ⁹⁸, M. Heller ²⁹, S. Hellman ^{146a,146b}, D. Hellmich ²⁰, C. Helsens ¹¹, R.C.W. Henderson ⁷¹, M. Henke ^{58a}, A. Henrichs ⁵⁴, A.M. Henriques Correia ²⁹, S. Henrot-Versille ¹¹⁵, C. Hensel ⁵⁴, T. Henß ¹⁷⁵, C.M. Hernandez ⁷, Y. Hernández Jiménez ¹⁶⁷, R. Herrberg ¹⁵, G. Herten ⁴⁸, R. Hertenberger ⁹⁸, L. Hervas ²⁹, G.G. Hesketh ⁷⁷, N.P. Hessey ¹⁰⁵, E. Higón-Rodriguez ¹⁶⁷, J.C. Hill ²⁷, K.H. Hiller ⁴¹, S. Hillert ²⁰, S.J. Hillier ¹⁷, I. Hinchliffe ¹⁴, E. Hines ¹²⁰, M. Hirose ¹¹⁶, F. Hirsch ⁴², D. Hirschbuehl ¹⁷⁵, J. Hobbs ¹⁴⁸, N. Hod ¹⁵³, M.C. Hodgkinson ¹³⁹, P. Hodgson ¹³⁹, A. Hoecker ²⁹, M.R. Hoeferkamp ¹⁰³, J. Hoffman ³⁹, D. Hoffmann ⁸³, M. Hohlfeld ⁸¹, M. Holder ¹⁴¹, S.O. Holmgren ^{146a}, T. Holy ¹²⁷, J.L. Holzbauer ⁸⁸, T.M. Hong ¹²⁰, L. Hooft van Huysduynen ¹⁰⁸, C. Horn ¹⁴³, S. Horner ⁴⁸, J.-Y. Hostachy ⁵⁵, S. Hou ¹⁵¹, A. Hoummada ^{135a}, J. Howard ¹¹⁸, J. Howarth ⁸², I. Hristova ¹⁵, J. Hrvnac ¹¹⁵, T. Hryna'ova ⁴, P.J. Hsu ⁸¹, S.-C. Hsu ¹⁴, Z. Hubacek ¹²⁷, F. Hubaut ⁸³, F. Huegging ²⁰, A. Huettmann ⁴¹, T.B. Huffman ¹¹⁸, E.W. Hughes ³⁴, G. Hughes ⁷¹, M. Huhtinen ²⁹, M. Hurwitz ¹⁴, U. Husemann ⁴¹, N. Huseynov ^{64,r}, J. Huston ⁸⁸, J. Huth ⁵⁷, G. Iacobucci ⁴⁹, G. Iakovidis ⁹, M. Ibbotson ⁸², I. Ibragimov ¹⁴¹, L. Iconomou-Fayard ¹¹⁵, J. Idarraga ¹¹⁵, P. Iengo ^{102a}, O. Igolkina ¹⁰⁵, Y. Ikegami ⁶⁵, M. Ikeno ⁶⁵, D. Iliadis ¹⁵⁴, N. Ilic ¹⁵⁸, T. Ince ²⁰, J. Inigo-Golfin ²⁹, P. Ioannou ⁸, M. Iodice ^{134a}, K. Iordanidou ⁸, V. Ippolito ^{132a,132b}, A. Irles Quiles ¹⁶⁷, C. Isaksson ¹⁶⁶, M. Ishino ⁶⁷, M. Ishitsuka ¹⁵⁷, R. Ishmukhametov ³⁹, C. Issever ¹¹⁸, S. Istin ^{18a}, A.V. Ivashin ¹²⁸, W. Iwanski ³⁸, H. Iwasaki ⁶⁵, J.M. Izen ⁴⁰, V. Izzo ^{102a}, B. Jackson ¹²⁰, J.N. Jackson ⁷³, P. Jackson ¹⁴³, M.R. Jaekel ²⁹, V. Jain ⁶⁰, K. Jakobs ⁴⁸, S. Jakobsen ³⁵, T. Jakoubek ¹²⁵, J. Jakubek ¹²⁷, D.K. Jana ¹¹¹, E. Jansen ⁷⁷, H. Jansen ²⁹, A. Jantsch ⁹⁹, M. Janus ⁴⁸, G. Jarlskog ⁷⁹, L. Jeanty ⁵⁷, I. Jen-La Plante ³⁰, P. Jenni ²⁹, A. Jeremie ⁴, P. Jež ³⁵, S. Jézéquel ⁴, M.K. Jha ^{19a}, H. Ji ¹⁷³, W. Ji ⁸¹, J. Jia ¹⁴⁸, Y. Jiang ^{32b}, M. Jimenez Belenguer ⁴¹, S. Jin ^{32a}, O. Jinnouchi ¹⁵⁷, M.D. Joergensen ³⁵, D. Joffe ³⁹, M. Johansen ^{146a,146b}, K.E. Johansson ^{146a}, P. Johansson ¹³⁹, S. Johnert ⁴¹, K.A. Johns ⁶, K. Jon-And ^{146a,146b}, G. Jones ¹⁷⁰, R.W.L. Jones ⁷¹, T.J. Jones ⁷³, C. Joram ²⁹, P.M. Jorge ^{124a}, K.D. Joshi ⁸², J. Jovicevic ¹⁴⁷, T. Jovin ^{12b}, X. Ju ¹⁷³, C.A. Jung ⁴², R.M. Jungst ²⁹, V. Juraneck ¹²⁵, P. Jussel ⁶¹, A. Juste Rozas ¹¹, S. Kabana ¹⁶, M. Kaci ¹⁶⁷, A. Kaczmarska ³⁸, P. Kadlecik ³⁵, M. Kado ¹¹⁵, H. Kagan ¹⁰⁹, M. Kagan ⁵⁷, E. Kajomovitz ¹⁵², S. Kalinin ¹⁷⁵, L.V. Kalinovskaya ⁶⁴, S. Kama ³⁹, N. Kanaya ¹⁵⁵, M. Kaneda ²⁹, S. Kaneti ²⁷, T. Kanno ¹⁵⁷, V.A. Kantserov ⁹⁶, J. Kanzaki ⁶⁵, B. Kaplan ¹⁷⁶, A. Kapliy ³⁰, J. Kaplon ²⁹, D. Kar ⁵³, M. Karagounis ²⁰, K. Karakostas ⁹, M. Karnevskiy ⁴¹, V. Kartvelishvili ⁷¹, A.N. Karyukhin ¹²⁸, L. Kashif ¹⁷³, G. Kasieczka ^{58b}, R.D. Kass ¹⁰⁹, A. Kastanas ¹³, M. Kataoka ⁴, Y. Kataoka ¹⁵⁵, E. Katsoufis ⁹, J. Katzy ⁴¹, V. Kaushik ⁶, K. Kawagoe ⁶⁹, T. Kawamoto ¹⁵⁵, G. Kawamura ⁸¹, M.S. Kayl ¹⁰⁵, V.A. Kazanin ¹⁰⁷, M.Y. Kazarinov ⁶⁴, R. Keeler ¹⁶⁹, R. Kehoe ³⁹, M. Keil ⁵⁴, G.D. Kekelidze ⁶⁴, J.S. Keller ¹³⁸, M. Kenyon ⁵³, O. Kepka ¹²⁵, N. Kerschen ²⁹, B.P. Kerševan ⁷⁴, S. Kersten ¹⁷⁵, K. Kessoku ¹⁵⁵, J. Keung ¹⁵⁸, F. Khalil-zada ¹⁰, H. Khandanyan ¹⁶⁵, A. Khanov ¹¹², D. Kharchenko ⁶⁴, A. Khodinov ⁹⁶, A. Khomich ^{58a}, T.J. Khoo ²⁷, G. Khoriauli ²⁰, A. Khoroshilov ¹⁷⁵, V. Khovanskiy ⁹⁵, E. Khramov ⁶⁴, J. Khubua ^{51b}, H. Kim ^{146a,146b}, S.H. Kim ¹⁶⁰, N. Kimura ¹⁷¹, O. Kind ¹⁵, B.T. King ⁷³, M. King ⁶⁶, R.S.B. King ¹¹⁸, J. Kirk ¹²⁹, A.E. Kiryunin ⁹⁹, T. Kishimoto ⁶⁶, D. Kisielewska ³⁷, T. Kittelmann ¹²³, E. Kladiva ^{144b}, M. Klein ⁷³, U. Klein ⁷³, K. Kleinknecht ⁸¹, M. Klemetti ⁸⁵, A. Klier ¹⁷², P. Klimek ^{146a,146b}, A. Klimentov ²⁴, R. Klingenberg ⁴², J.A. Klinger ⁸², E.B. Klinkby ³⁵, T. Klioutchnikova ²⁹, P.F. Klok ¹⁰⁴, S. Klous ¹⁰⁵, E.-E. Kluge ^{58a}, T. Kluge ⁷³, P. Kluit ¹⁰⁵, S. Kluth ⁹⁹, N.S. Knecht ¹⁵⁸, E. Kneringer ⁶¹, E.B.F.G. Knoops ⁸³, A. Knue ⁵⁴, B.R. Ko ⁴⁴, T. Kobayashi ¹⁵⁵, M. Kobel ⁴³, M. Kocian ¹⁴³, P. Kodys ¹²⁶, K. Köneke ²⁹, A.C. König ¹⁰⁴, S. Koenig ⁸¹, L. Köpke ⁸¹, F. Koetsveld ¹⁰⁴, P. Koevesarki ²⁰, T. Koffas ²⁸, E. Koffeman ¹⁰⁵, L.A. Kogan ¹¹⁸, S. Kohlmann ¹⁷⁵, F. Kohn ⁵⁴, Z. Kohout ¹²⁷, T. Kohriki ⁶⁵, T. Koi ¹⁴³, G.M. Kolachev ¹⁰⁷, H. Kolanoski ¹⁵, V. Kolesnikov ⁶⁴, I. Koletsou ^{89a}, J. Koll ⁸⁸, M. Kollefrath ⁴⁸, A.A. Komar ⁹⁴, Y. Komori ¹⁵⁵, T. Kondo ⁶⁵, T. Kono ^{41,s},

- A.I. Kononov⁴⁸, R. Konoplich^{108,t}, N. Konstantinidis⁷⁷, S. Koperny³⁷, K. Korcyl³⁸, K. Kordas¹⁵⁴,
 A. Korn¹¹⁸, A. Korol¹⁰⁷, I. Korolkov¹¹, E.V. Korolkova¹³⁹, V.A. Korotkov¹²⁸, O. Kortner⁹⁹, S. Kortner⁹⁹,
 V.V. Kostyukhin²⁰, S. Kotov⁹⁹, V.M. Kotov⁶⁴, A. Kotwal⁴⁴, C. Kourkoumelis⁸, V. Kouskoura¹⁵⁴,
 A. Koutsman^{159a}, R. Kowalewski¹⁶⁹, T.Z. Kowalski³⁷, W. Kozanecki¹³⁶, A.S. Kozhin¹²⁸, V. Kral¹²⁷,
 V.A. Kramarenko⁹⁷, G. Kramberger⁷⁴, M.W. Krasny⁷⁸, A. Krasznahorkay¹⁰⁸, J. Kraus⁸⁸, J.K. Kraus²⁰,
 S. Kreiss¹⁰⁸, F. Krejci¹²⁷, J. Kretzschmar⁷³, N. Krieger⁵⁴, P. Krieger¹⁵⁸, K. Kroeninger⁵⁴, H. Kroha⁹⁹,
 J. Kroll¹²⁰, J. Kroeseberg²⁰, J. Krstic^{12a}, U. Kruchonak⁶⁴, H. Krüger²⁰, T. Kruker¹⁶, N. Krumnack⁶³,
 Z.V. Krumshteyn⁶⁴, A. Kruth²⁰, T. Kubota⁸⁶, S. Kuday^{3a}, S. Kuehn⁴⁸, A. Kugel^{58c}, T. Kuhl⁴¹, D. Kuhn⁶¹,
 V. Kukhtin⁶⁴, Y. Kulchitsky⁹⁰, S. Kuleshov^{31b}, C. Kummer⁹⁸, M. Kuna⁷⁸, J. Kunkle¹²⁰, A. Kupco¹²⁵,
 H. Kurashige⁶⁶, M. Kurata¹⁶⁰, Y.A. Kurochkin⁹⁰, V. Kus¹²⁵, E.S. Kuwertz¹⁴⁷, M. Kuze¹⁵⁷, J. Kvita¹⁴²,
 R. Kwee¹⁵, A. La Rosa⁴⁹, L. La Rotonda^{36a,36b}, L. Labarga⁸⁰, J. Labbe⁴, S. Lablak^{135a}, C. Lacasta¹⁶⁷,
 F. Lacava^{132a,132b}, H. Lacker¹⁵, D. Lacour⁷⁸, V.R. Lacuesta¹⁶⁷, E. Ladygin⁶⁴, R. Lafaye⁴, B. Laforge⁷⁸,
 T. Lagouri⁸⁰, S. Lai⁴⁸, E. Laisne⁵⁵, M. Lamanna²⁹, L. Lambourne⁷⁷, C.L. Lampen⁶, W. Lampl⁶,
 E. Lancon¹³⁶, U. Landgraf⁴⁸, M.P.J. Landon⁷⁵, J.L. Lane⁸², V.S. Lang^{58a}, C. Lange⁴¹, A.J. Lankford¹⁶³,
 F. Lanni²⁴, K. Lantzsch¹⁷⁵, S. Laplace⁷⁸, C. Lapoire²⁰, J.F. Laporte¹³⁶, T. Lari^{89a}, A. Larner¹¹⁸,
 M. Lassnig²⁹, P. Laurelli⁴⁷, V. Lavorini^{36a,36b}, W. Lavrijisen¹⁴, P. Laycock⁷³, O. Le Dortz⁷⁸,
 E. Le Guiriec⁸³, C. Le Maner¹⁵⁸, E. Le Menedeu¹¹, T. LeCompte⁵, F. Ledroit-Guillon⁵⁵, H. Lee¹⁰⁵,
 J.S.H. Lee¹¹⁶, S.C. Lee¹⁵¹, L. Lee¹⁷⁶, M. Lefebvre¹⁶⁹, M. Legendre¹³⁶, F. Legger⁹⁸, C. Leggett¹⁴,
 M. Lehacher²⁰, G. Lehmann Miotto²⁹, X. Lei⁶, M.A.L. Leite^{23d}, R. Leitner¹²⁶, D. Lelloouch¹⁷²,
 B. Lemmer⁵⁴, V. Lendermann^{58a}, K.J.C. Leney^{145b}, T. Lenz¹⁰⁵, G. Lenzen¹⁷⁵, B. Lenzi²⁹, K. Leonhardt⁴³,
 S. Leontsinis⁹, F. Lepold^{58a}, C. Leroy⁹³, J.-R. Lessard¹⁶⁹, C.G. Lester²⁷, C.M. Lester¹²⁰, J. Levêque⁴,
 D. Levin⁸⁷, L.J. Levinson¹⁷², A. Lewis¹¹⁸, G.H. Lewis¹⁰⁸, A.M. Leyko²⁰, M. Leyton¹⁵, B. Li⁸³, H. Li^{173,u},
 S. Li^{32b,v}, X. Li⁸⁷, Z. Liang^{118,w}, H. Liao³³, B. Liberti^{133a}, P. Lichard²⁹, M. Lichtnecker⁹⁸, K. Lie¹⁶⁵,
 W. Liebig¹³, C. Limbach²⁰, A. Limosani⁸⁶, M. Limper⁶², S.C. Lin^{151,x}, F. Linde¹⁰⁵, J.T. Linnemann⁸⁸,
 E. Lipeles¹²⁰, A. Lipniacka¹³, T.M. Liss¹⁶⁵, D. Lissauer²⁴, A. Lister⁴⁹, A.M. Litke¹³⁷, C. Liu²⁸, D. Liu¹⁵¹,
 H. Liu⁸⁷, J.B. Liu⁸⁷, L. Liu⁸⁷, M. Liu^{32b}, Y. Liu^{32b}, M. Livan^{119a,119b}, S.S.A. Livermore¹¹⁸, A. Lleres⁵⁵,
 J. Llorente Merino⁸⁰, S.L. Lloyd⁷⁵, E. Lobodzinska⁴¹, P. Loch⁶, W.S. Lockman¹³⁷, T. Loddenkoetter²⁰,
 F.K. Loebinger⁸², A. Loginov¹⁷⁶, C.W. Loh¹⁶⁸, T. Lohse¹⁵, K. Lohwasser⁴⁸, M. Lokajicek¹²⁵,
 V.P. Lombardo⁴, R.E. Long⁷¹, L. Lopes^{124a}, D. Lopez Mateos⁵⁷, J. Lorenz⁹⁸, N. Lorenzo Martinez¹¹⁵,
 M. Losada¹⁶², P. Loscutoff¹⁴, F. Lo Sterzo^{132a,132b}, M.J. Losty^{159a}, X. Lou⁴⁰, A. Lounis¹¹⁵, K.F. Loureiro¹⁶²,
 J. Love²¹, P.A. Love⁷¹, A.J. Lowe^{143,e}, F. Lu^{32a}, H.J. Lubatti¹³⁸, C. Luci^{132a,132b}, A. Lucotte⁵⁵, A. Ludwig⁴³,
 D. Ludwig⁴¹, I. Ludwig⁴⁸, J. Ludwig⁴⁸, F. Luehring⁶⁰, G. Luijckx¹⁰⁵, W. Lukas⁶¹, D. Lumb⁴⁸,
 L. Luminari^{132a}, E. Lund¹¹⁷, B. Lund-Jensen¹⁴⁷, B. Lundberg⁷⁹, J. Lundberg^{146a,146b},
 O. Lundberg^{146a,146b}, J. Lundquist³⁵, M. Lungwitz⁸¹, D. Lynn²⁴, E. Lytken⁷⁹, H. Ma²⁴, L.L. Ma¹⁷³,
 G. Maccarrone⁴⁷, A. Macchiolo⁹⁹, B. Maček⁷⁴, J. Machado Miguens^{124a}, R. Mackeprang³⁵,
 R.J. Madaras¹⁴, W.F. Mader⁴³, R. Maenner^{58c}, T. Maeno²⁴, P. Mättig¹⁷⁵, S. Mättig⁴¹, L. Magnoni²⁹,
 E. Magradze⁵⁴, K. Mahboubi⁴⁸, S. Mahmoud⁷³, G. Mahout¹⁷, C. Maiani¹³⁶, C. Maidantchik^{23a},
 A. Maio^{124a,b}, S. Majewski²⁴, Y. Makida⁶⁵, N. Makovec¹¹⁵, P. Mal¹³⁶, B. Malaescu²⁹, Pa. Malecki³⁸,
 P. Malecki³⁸, V.P. Maleev¹²¹, F. Malek⁵⁵, U. Mallik⁶², D. Malon⁵, C. Malone¹⁴³, S. Maltezos⁹,
 V. Malyshев¹⁰⁷, S. Malyukov²⁹, R. Mameghani⁹⁸, J. Mamuzic^{12b}, A. Manabe⁶⁵, L. Mandelli^{89a},
 I. Mandić⁷⁴, R. Mandrysch¹⁵, J. Maneira^{124a}, P.S. Mangeard⁸⁸, L. Manhaes de Andrade Filho^{23a},
 A. Mann⁵⁴, P.M. Manning¹³⁷, A. Manousakis-Katsikakis⁸, B. Mansoulie¹³⁶, A. Mapelli²⁹, L. Mapelli²⁹,
 L. March⁸⁰, J.F. Marchand²⁸, F. Marchese^{133a,133b}, G. Marchiori⁷⁸, M. Marcisovsky¹²⁵, C.P. Marino¹⁶⁹,
 F. Marroquim^{23a}, Z. Marshall²⁹, F.K. Martens¹⁵⁸, L.F. Marti¹⁶, S. Marti-Garcia¹⁶⁷, B. Martin²⁹,
 B. Martin⁸⁸, J.P. Martin⁹³, T.A. Martin¹⁷, V.J. Martin⁴⁵, B. Martin dit Latour⁴⁹, S. Martin-Haugh¹⁴⁹,
 M. Martinez¹¹, V. Martinez Outschoorn⁵⁷, A.C. Martyniuk¹⁶⁹, M. Marx⁸², F. Marzano^{132a}, A. Marzin¹¹¹,
 L. Masetti⁸¹, T. Mashimo¹⁵⁵, R. Mashinistov⁹⁴, J. Masik⁸², A.L. Maslennikov¹⁰⁷, I. Massa^{19a,19b},
 G. Massaro¹⁰⁵, N. Massol⁴, A. Mastroberardino^{36a,36b}, T. Masubuchi¹⁵⁵, P. Matricon¹¹⁵,
 H. Matsunaga¹⁵⁵, T. Matsushita⁶⁶, C. Mattravers^{118,c}, J. Maurer⁸³, S.J. Maxfield⁷³, A. Mayne¹³⁹,
 R. Mazini¹⁵¹, M. Mazur²⁰, L. Mazzaferro^{133a,133b}, M. Mazzanti^{89a}, S.P. Mc Kee⁸⁷, A. McCarn¹⁶⁵,
 R.L. McCarthy¹⁴⁸, T.G. McCarthy²⁸, N.A. McCubbin¹²⁹, K.W. McFarlane⁵⁶, J.A. McFayden¹³⁹,
 H. McGlone⁵³, G. Mchedlidze^{51b}, T. McLaughlan¹⁷, S.J. McMahon¹²⁹, R.A. McPherson^{169,k}, A. Meade⁸⁴,

- J. Mechnick ¹⁰⁵, M. Mechtel ¹⁷⁵, M. Medinnis ⁴¹, R. Meera-Lebbai ¹¹¹, T. Meguro ¹¹⁶, R. Mehdiyev ⁹³, S. Mehlhase ³⁵, A. Mehta ⁷³, K. Meier ^{58a}, B. Meirose ⁷⁹, C. Melachrinos ³⁰, B.R. Mellado Garcia ¹⁷³, F. Meloni ^{89a,89b}, L. Mendoza Navas ¹⁶², Z. Meng ^{151,u}, A. Mengarelli ^{19a,19b}, S. Menke ⁹⁹, E. Meoni ¹⁶¹, K.M. Mercurio ⁵⁷, P. Mermod ⁴⁹, L. Merola ^{102a,102b}, C. Meroni ^{89a}, F.S. Merritt ³⁰, H. Merritt ¹⁰⁹, A. Messina ^{29,y}, J. Metcalfe ¹⁰³, A.S. Mete ¹⁶³, C. Meyer ⁸¹, C. Meyer ³⁰, J.-P. Meyer ¹³⁶, J. Meyer ¹⁷⁴, J. Meyer ⁵⁴, T.C. Meyer ²⁹, W.T. Meyer ⁶³, J. Miao ^{32d}, S. Michal ²⁹, L. Micu ^{25a}, R.P. Middleton ¹²⁹, S. Migas ⁷³, L. Mijović ¹³⁶, G. Mikenberg ¹⁷², M. Mikestikova ¹²⁵, M. Mikuž ⁷⁴, D.W. Miller ³⁰, R.J. Miller ⁸⁸, W.J. Mills ¹⁶⁸, C. Mills ⁵⁷, A. Milov ¹⁷², D.A. Milstead ^{146a,146b}, D. Milstein ¹⁷², A.A. Minaenko ¹²⁸, M. Miñano Moya ¹⁶⁷, I.A. Minashvili ⁶⁴, A.I. Mincer ¹⁰⁸, B. Mindur ³⁷, M. Mineev ⁶⁴, Y. Ming ¹⁷³, L.M. Mir ¹¹, G. Mirabelli ^{132a}, J. Mitrevski ¹³⁷, V.A. Mitsou ¹⁶⁷, S. Mitsui ⁶⁵, P.S. Miyagawa ¹³⁹, J.U. Mjörnmark ⁷⁹, T. Moa ^{146a,146b}, V. Moeller ²⁷, K. Möning ⁴¹, N. Möser ²⁰, S. Mohapatra ¹⁴⁸, W. Mohr ⁴⁸, R. Moles-Valls ¹⁶⁷, J. Monk ⁷⁷, E. Monnier ⁸³, J. Montejo Berlingen ¹¹, S. Montesano ^{89a,89b}, F. Monticelli ⁷⁰, S. Monzani ^{19a,19b}, R.W. Moore ², G.F. Moorhead ⁸⁶, C. Mora Herrera ⁴⁹, A. Moraes ⁵³, N. Morange ¹³⁶, J. Morel ⁵⁴, G. Morello ^{36a,36b}, D. Moreno ⁸¹, M. Moreno Llácer ¹⁶⁷, P. Morettini ^{50a}, M. Morgenstern ⁴³, M. Morii ⁵⁷, A.K. Morley ²⁹, G. Mornacchi ²⁹, J.D. Morris ⁷⁵, L. Morvaj ¹⁰¹, H.G. Moser ⁹⁹, M. Mosidze ^{51b}, J. Moss ¹⁰⁹, R. Mount ¹⁴³, E. Mountricha ^{9,z}, S.V. Mouraviev ⁹⁴, E.J.W. Moyse ⁸⁴, F. Mueller ^{58a}, J. Mueller ¹²³, K. Mueller ²⁰, T.A. Müller ⁹⁸, T. Mueller ⁸¹, D. Muenstermann ²⁹, Y. Munwes ¹⁵³, W.J. Murray ¹²⁹, I. Mussche ¹⁰⁵, E. Musto ^{102a,102b}, A.G. Myagkov ¹²⁸, M. Myska ¹²⁵, J. Nadal ¹¹, K. Nagai ¹⁶⁰, K. Nagano ⁶⁵, A. Nagarkar ¹⁰⁹, Y. Nagasaka ⁵⁹, M. Nagel ⁹⁹, A.M. Nairz ²⁹, Y. Nakahama ²⁹, K. Nakamura ¹⁵⁵, T. Nakamura ¹⁵⁵, I. Nakano ¹¹⁰, G. Nanava ²⁰, A. Napier ¹⁶¹, R. Narayan ^{58b}, M. Nash ^{77,c}, T. Nattermann ²⁰, T. Naumann ⁴¹, G. Navarro ¹⁶², H.A. Neal ⁸⁷, P.Yu. Nechaeva ⁹⁴, T.J. Neep ⁸², A. Negri ^{119a,119b}, G. Negri ²⁹, S. Nektarijevic ⁴⁹, A. Nelson ¹⁶³, T.K. Nelson ¹⁴³, S. Nemecek ¹²⁵, P. Nemethy ¹⁰⁸, A.A. Nepomuceno ^{23a}, M. Nessi ^{29,aa}, M.S. Neubauer ¹⁶⁵, A. Neusiedl ⁸¹, R.M. Neves ¹⁰⁸, P. Nevski ²⁴, P.R. Newman ¹⁷, V. Nguyen Thi Hong ¹³⁶, R.B. Nickerson ¹¹⁸, R. Nicolaïdou ¹³⁶, B. Nicquevert ²⁹, F. Niedercorn ¹¹⁵, J. Nielsen ¹³⁷, N. Nikiforou ³⁴, A. Nikiforov ¹⁵, V. Nikolaenko ¹²⁸, I. Nikolic-Audit ⁷⁸, K. Nikolic ⁴⁹, K. Nikolopoulos ²⁴, H. Nilsen ⁴⁸, P. Nilsson ⁷, Y. Ninomiya ¹⁵⁵, A. Nisati ^{132a}, R. Nisius ⁹⁹, T. Nobe ¹⁵⁷, L. Nodulman ⁵, M. Nomachi ¹¹⁶, I. Nomidis ¹⁵⁴, M. Nordberg ²⁹, P.R. Norton ¹²⁹, J. Novakova ¹²⁶, M. Nozaki ⁶⁵, L. Nozka ¹¹³, I.M. Nugent ^{159a}, A.-E. Nuncio-Quiroz ²⁰, G. Nunes Hanninger ⁸⁶, T. Nunnemann ⁹⁸, E. Nurse ⁷⁷, B.J. O'Brien ⁴⁵, S.W. O'Neale ^{17,*}, D.C. O'Neil ¹⁴², V. O'Shea ⁵³, L.B. Oakes ⁹⁸, F.G. Oakham ^{28,d}, H. Oberlack ⁹⁹, J. Ocariz ⁷⁸, A. Ochi ⁶⁶, S. Oda ⁶⁹, S. Odaka ⁶⁵, J. Odier ⁸³, H. Ogren ⁶⁰, A. Oh ⁸², S.H. Oh ⁴⁴, C.C. Ohm ^{146a,146b}, T. Ohshima ¹⁰¹, H. Okawa ¹⁶³, Y. Okumura ³⁰, T. Okuyama ¹⁵⁵, A. Olariu ^{25a}, A.G. Olchevski ⁶⁴, S.A. Olivares Pino ^{31a}, M. Oliveira ^{124a,h}, D. Oliveira Damazio ²⁴, E. Oliver Garcia ¹⁶⁷, D. Olivito ¹²⁰, A. Olszewski ³⁸, J. Olszowska ³⁸, A. Onofre ^{124a,ab}, P.U.E. Onyisi ³⁰, C.J. Oram ^{159a}, M.J. Oreglia ³⁰, Y. Oren ¹⁵³, D. Orestano ^{134a,134b}, N. Orlando ^{72a,72b}, I. Orlov ¹⁰⁷, C. Oropeza Barrera ⁵³, R.S. Orr ¹⁵⁸, B. Osculati ^{50a,50b}, R. Ospanov ¹²⁰, C. Osuna ¹¹, G. Otero y Garzon ²⁶, J.P. Ottersbach ¹⁰⁵, M. Ouchrif ^{135d}, E.A. Ouellette ¹⁶⁹, F. Ould-Saada ¹¹⁷, A. Ouraou ¹³⁶, Q. Ouyang ^{32a}, A. Ovcharova ¹⁴, M. Owen ⁸², S. Owen ¹³⁹, V.E. Ozcan ^{18a}, N. Ozturk ⁷, A. Pacheco Pages ¹¹, C. Padilla Aranda ¹¹, S. Pagan Griso ¹⁴, E. Paganis ¹³⁹, F. Paige ²⁴, P. Pais ⁸⁴, K. Pajchel ¹¹⁷, G. Palacino ^{159b}, C.P. Paleari ⁶, S. Palestini ²⁹, D. Pallin ³³, A. Palma ^{124a}, J.D. Palmer ¹⁷, Y.B. Pan ¹⁷³, E. Panagiotopoulou ⁹, P. Pani ¹⁰⁵, N. Panikashvili ⁸⁷, S. Panitkin ²⁴, D. Pantea ^{25a}, A. Papadelis ^{146a}, Th.D. Papadopoulou ⁹, A. Paramonov ⁵, D. Paredes Hernandez ³³, W. Park ^{24,ac}, M.A. Parker ²⁷, F. Parodi ^{50a,50b}, J.A. Parsons ³⁴, U. Parzefall ⁴⁸, S. Pashapour ⁵⁴, E. Pasqualucci ^{132a}, S. Passaggio ^{50a}, A. Passeri ^{134a}, F. Pastore ^{134a,134b}, Fr. Pastore ⁷⁶, G. Pásztor ^{49,ad}, S. Pataraia ¹⁷⁵, N. Patel ¹⁵⁰, J.R. Pater ⁸², S. Patricelli ^{102a,102b}, T. Pauly ²⁹, M. Pecsy ^{144a}, M.I. Pedraza Morales ¹⁷³, S.V. Peleganchuk ¹⁰⁷, D. Pelikan ¹⁶⁶, H. Peng ^{32b}, B. Penning ³⁰, A. Penson ³⁴, J. Penwell ⁶⁰, M. Perantoni ^{23a}, K. Perez ^{34,ae}, T. Perez Cavalcanti ⁴¹, E. Perez Codina ^{159a}, M.T. Pérez García-Estañ ¹⁶⁷, V. Perez Reale ³⁴, L. Perini ^{89a,89b}, H. Pernegger ²⁹, R. Perrino ^{72a}, P. Perrodo ⁴, V.D. Peshekhonov ⁶⁴, K. Peters ²⁹, B.A. Petersen ²⁹, J. Petersen ²⁹, T.C. Petersen ³⁵, E. Petit ⁴, A. Petridis ¹⁵⁴, C. Petridou ¹⁵⁴, E. Petrolo ^{132a}, F. Petracci ^{134a,134b}, D. Petschull ⁴¹, M. Petteni ¹⁴², R. Pezoa ^{31b}, A. Phan ⁸⁶, P.W. Phillips ¹²⁹, G. Piacquadio ²⁹, A. Picazio ⁴⁹, E. Piccaro ⁷⁵, M. Piccinini ^{19a,19b}, S.M. Piec ⁴¹, R. Piegaia ²⁶, D.T. Pignotti ¹⁰⁹, J.E. Pilcher ³⁰, A.D. Pilkington ⁸², J. Pina ^{124a,b}, M. Pinamonti ^{164a,164c}, A. Pinder ¹¹⁸, J.L. Pinfold ², B. Pinto ^{124a}, C. Pizio ^{89a,89b}, M. Plamondon ¹⁶⁹, M.-A. Pleier ²⁴, E. Plotnikova ⁶⁴, A. Poblaguev ²⁴, S. Poddar ^{58a}, F. Podlyski ³³, L. Poggioli ¹¹⁵, T. Poghosyan ²⁰, M. Pohl ⁴⁹, G. Polesello ^{119a},

- A. Policicchio ^{36a,36b}, A. Polini ^{19a}, J. Poll ⁷⁵, V. Polychronakos ²⁴, D. Pomeroy ²², K. Pommès ²⁹,
 L. Pontecorvo ^{132a}, B.G. Pope ⁸⁸, G.A. Popeneciu ^{25a}, D.S. Popovic ^{12a}, A. Poppleton ²⁹, X. Portell Bueso ²⁹,
 G.E. Pospelov ⁹⁹, S. Pospisil ¹²⁷, I.N. Potrap ⁹⁹, C.J. Potter ¹⁴⁹, C.T. Potter ¹¹⁴, G. Poulard ²⁹, J. Poveda ⁶⁰,
 V. Pozdnyakov ⁶⁴, R. Prabhu ⁷⁷, P. Pralavorio ⁸³, A. Pranko ¹⁴, S. Prasad ²⁹, R. Pravahan ²⁴, S. Prell ⁶³,
 K. Pretzl ¹⁶, D. Price ⁶⁰, J. Price ⁷³, L.E. Price ⁵, D. Prieur ¹²³, M. Primavera ^{72a}, K. Prokofiev ¹⁰⁸,
 F. Prokoshin ^{31b}, S. Protopopescu ²⁴, J. Proudfoot ⁵, X. Prudent ⁴³, M. Przybycien ³⁷, H. Przysiezniak ⁴,
 S. Psoroulas ²⁰, E. Ptacek ¹¹⁴, E. Pueschel ⁸⁴, J. Purdham ⁸⁷, M. Purohit ^{24,ac}, P. Puzo ¹¹⁵, Y. Pylypchenko ⁶²,
 J. Qian ⁸⁷, A. Quadt ⁵⁴, D.R. Quarrie ¹⁴, W.B. Quayle ¹⁷³, F. Quinonez ^{31a}, M. Raas ¹⁰⁴, V. Radescu ⁴¹,
 P. Radloff ¹¹⁴, T. Rador ^{18a}, F. Ragusa ^{89a,89b}, G. Rahal ¹⁷⁸, A.M. Rahimi ¹⁰⁹, D. Rahm ²⁴, S. Rajagopalan ²⁴,
 M. Rammensee ⁴⁸, M. Rammes ¹⁴¹, A.S. Randle-Conde ³⁹, K. Randrianarivony ²⁸, F. Rauscher ⁹⁸,
 T.C. Rave ⁴⁸, M. Raymond ²⁹, A.L. Read ¹¹⁷, D.M. Rebuzzi ^{119a,119b}, A. Redelbach ¹⁷⁴, G. Redlinger ²⁴,
 R. Reece ¹²⁰, K. Reeves ⁴⁰, E. Reinherz-Aronis ¹⁵³, A. Reinsch ¹¹⁴, I. Reisinger ⁴², C. Rembser ²⁹, Z.L. Ren ¹⁵¹,
 A. Renaud ¹¹⁵, M. Rescigno ^{132a}, S. Resconi ^{89a}, B. Resende ¹³⁶, P. Reznicek ⁹⁸, R. Rezvani ¹⁵⁸, R. Richter ⁹⁹,
 E. Richter-Was ⁴, M. Ridel ⁷⁸, M. Rijpstra ¹⁰⁵, M. Rijssenbeek ¹⁴⁸, A. Rimoldi ^{119a,119b}, L. Rinaldi ^{19a},
 R.R. Rios ³⁹, I. Riu ¹¹, G. Rivoltella ^{89a,89b}, F. Rizatdinova ¹¹², E. Rizvi ⁷⁵, S.H. Robertson ^{85,k},
 A. Robichaud-Veronneau ¹¹⁸, D. Robinson ²⁷, J.E.M. Robinson ⁷⁷, A. Robson ⁵³, J.G. Rocha de Lima ¹⁰⁶,
 C. Roda ^{122a,122b}, D. Roda Dos Santos ²⁹, A. Roe ⁵⁴, S. Roe ²⁹, O. Røhne ¹¹⁷, S. Rolli ¹⁶¹, A. Romaniouk ⁹⁶,
 M. Romano ^{19a,19b}, G. Romeo ²⁶, E. Romero Adam ¹⁶⁷, L. Roos ⁷⁸, E. Ros ¹⁶⁷, S. Rosati ^{132a}, K. Rosbach ⁴⁹,
 A. Rose ¹⁴⁹, M. Rose ⁷⁶, G.A. Rosenbaum ¹⁵⁸, E.I. Rosenberg ⁶³, P.L. Rosendahl ¹³, O. Rosenthal ¹⁴¹,
 L. Rosselet ⁴⁹, V. Rossetti ¹¹, E. Rossi ^{132a,132b}, L.P. Rossi ^{50a}, M. Rotaru ^{25a}, I. Roth ¹⁷², J. Rothberg ¹³⁸,
 D. Rousseau ¹¹⁵, C.R. Royon ¹³⁶, A. Rozanov ⁸³, Y. Rozen ¹⁵², X. Ruan ^{32a,af}, F. Rubbo ¹¹, I. Rubinskiy ⁴¹,
 B. Ruckert ⁹⁸, N. Ruckstuhl ¹⁰⁵, V.I. Rud ⁹⁷, C. Rudolph ⁴³, G. Rudolph ⁶¹, F. Rühr ⁶, A. Ruiz-Martinez ⁶³,
 L. Rumyantsev ⁶⁴, Z. Rurikova ⁴⁸, N.A. Rusakovich ⁶⁴, J.P. Rutherford ⁶, C. Ruwiedel ¹⁴, P. Ruzicka ¹²⁵,
 Y.F. Ryabov ¹²¹, P. Ryan ⁸⁸, M. Rybar ¹²⁶, G. Rybkin ¹¹⁵, N.C. Ryder ¹¹⁸, A.F. Saavedra ¹⁵⁰, I. Sadeh ¹⁵³,
 H.F.-W. Sadrozinski ¹³⁷, R. Sadykov ⁶⁴, F. Safai Tehrani ^{132a}, H. Sakamoto ¹⁵⁵, G. Salamanna ⁷⁵,
 A. Salamon ^{133a}, M. Saleem ¹¹¹, D. Salek ²⁹, D. Salihagic ⁹⁹, A. Salnikov ¹⁴³, J. Salt ¹⁶⁷,
 B.M. Salvachua Ferrando ⁵, D. Salvatore ^{36a,36b}, F. Salvatore ¹⁴⁹, A. Salvucci ¹⁰⁴, A. Salzburger ²⁹,
 D. Sampsonidis ¹⁵⁴, B.H. Samset ¹¹⁷, A. Sanchez ^{102a,102b}, V. Sanchez Martinez ¹⁶⁷, H. Sandaker ¹³,
 H.G. Sander ⁸¹, M.P. Sanders ⁹⁸, M. Sandhoff ¹⁷⁵, T. Sandoval ²⁷, C. Sandoval ¹⁶², R. Sandstroem ⁹⁹,
 D.P.C. Sankey ¹²⁹, A. Sansoni ⁴⁷, C. Santamarina Rios ⁸⁵, C. Santoni ³³, R. Santonico ^{133a,133b}, H. Santos ^{124a},
 J.G. Saraiva ^{124a}, T. Sarangi ¹⁷³, E. Sarkisyan-Grinbaum ⁷, F. Sarri ^{122a,122b}, G. Sartisohn ¹⁷⁵, O. Sasaki ⁶⁵,
 N. Sasao ⁶⁷, I. Satsounkevitch ⁹⁰, G. Sauvage ⁴, E. Sauvan ⁴, J.B. Sauvan ¹¹⁵, P. Savard ^{158,d}, V. Savinov ¹²³,
 D.O. Savu ²⁹, L. Sawyer ^{24,m}, D.H. Saxon ⁵³, J. Saxon ¹²⁰, C. Sbarra ^{19a}, A. Sbrizzi ^{19a,19b}, O. Scallon ⁹³,
 D.A. Scannicchio ¹⁶³, M. Scarcella ¹⁵⁰, J. Schaarschmidt ¹¹⁵, P. Schacht ⁹⁹, D. Schaefer ¹²⁰, U. Schäfer ⁸¹,
 S. Schaepe ²⁰, S. Schaetzl ^{58b}, A.C. Schaffer ¹¹⁵, D. Schaile ⁹⁸, R.D. Schamberger ¹⁴⁸, A.G. Schamov ¹⁰⁷,
 V. Scharf ^{58a}, V.A. Schegelsky ¹²¹, D. Scheirich ⁸⁷, M. Schernau ¹⁶³, M.I. Scherzer ³⁴, C. Schiavi ^{50a,50b},
 J. Schieck ⁹⁸, M. Schioppa ^{36a,36b}, S. Schlenker ²⁹, E. Schmidt ⁴⁸, K. Schmieden ²⁰, C. Schmitt ⁸¹,
 S. Schmitt ^{58b}, M. Schmitz ²⁰, B. Schneider ¹⁶, U. Schnoor ⁴³, A. Schöning ^{58b}, A.L.S. Schorlemmer ⁵⁴,
 M. Schott ²⁹, D. Schouten ^{159a}, J. Schovancova ¹²⁵, M. Schram ⁸⁵, C. Schroeder ⁸¹, N. Schroer ^{58c},
 M.J. Schultens ²⁰, J. Schultes ¹⁷⁵, H.-C. Schultz-Coulon ^{58a}, H. Schulz ¹⁵, M. Schumacher ⁴⁸,
 B.A. Schumm ¹³⁷, Ph. Schune ¹³⁶, C. Schwanenberger ⁸², A. Schwartzman ¹⁴³, Ph. Schwemling ⁷⁸,
 R. Schwienhorst ⁸⁸, R. Schwierz ⁴³, J. Schwindling ¹³⁶, T. Schwindt ²⁰, M. Schwoerer ⁴, G. Sciolla ²²,
 W.G. Scott ¹²⁹, J. Searcy ¹¹⁴, G. Sedov ⁴¹, E. Sedykh ¹²¹, S.C. Seidel ¹⁰³, A. Seiden ¹³⁷, F. Seifert ⁴³,
 J.M. Seixas ^{23a}, G. Sekhniaidze ^{102a}, S.J. Sekula ³⁹, K.E. Selbach ⁴⁵, D.M. Seliverstov ¹²¹, B. Sellden ^{146a},
 G. Sellers ⁷³, M. Seman ^{144b}, N. Semprini-Cesari ^{19a,19b}, C. Serfon ⁹⁸, L. Serin ¹¹⁵, L. Serkin ⁵⁴, R. Seuster ⁹⁹,
 H. Severini ¹¹¹, A. Sfyrla ²⁹, E. Shabalina ⁵⁴, M. Shamim ¹¹⁴, L.Y. Shan ^{32a}, J.T. Shank ²¹, Q.T. Shao ⁸⁶,
 M. Shapiro ¹⁴, P.B. Shatalov ⁹⁵, K. Shaw ^{164a,164c}, D. Sherman ¹⁷⁶, P. Sherwood ⁷⁷, A. Shibata ¹⁰⁸,
 S. Shimizu ²⁹, M. Shimojima ¹⁰⁰, T. Shin ⁵⁶, M. Shiyakova ⁶⁴, A. Shmeleva ⁹⁴, M.J. Shochet ³⁰, D. Short ¹¹⁸,
 S. Shrestha ⁶³, E. Shulga ⁹⁶, M.A. Shupe ⁶, P. Sicho ¹²⁵, A. Sidoti ^{132a}, F. Siegert ⁴⁸, Dj. Sijacki ^{12a},
 O. Silbert ¹⁷², J. Silva ^{124a}, Y. Silver ¹⁵³, D. Silverstein ¹⁴³, S.B. Silverstein ^{146a}, V. Simak ¹²⁷, O. Simard ¹³⁶,
 Lj. Simic ^{12a}, S. Simion ¹¹⁵, E. Simioni ⁸¹, B. Simmons ⁷⁷, R. Simoniello ^{89a,89b}, M. Simonyan ³⁵,
 P. Sinervo ¹⁵⁸, N.B. Sinev ¹¹⁴, V. Sipica ¹⁴¹, G. Siragusa ¹⁷⁴, A. Sircar ²⁴, A.N. Sisakyan ⁶⁴, S.Yu. Sivoklokov ⁹⁷,

- J. Sjölin ^{146a,146b}, T.B. Sjursen ¹³, L.A. Skinnari ¹⁴, H.P. Skottowe ⁵⁷, K. Skovpen ¹⁰⁷, P. Skubic ¹¹¹,
 M. Slater ¹⁷, T. Slavicek ¹²⁷, K. Sliwa ¹⁶¹, V. Smakhtin ¹⁷², B.H. Smart ⁴⁵, S.Yu. Smirnov ⁹⁶, Y. Smirnov ⁹⁶,
 L.N. Smirnova ⁹⁷, O. Smirnova ⁷⁹, B.C. Smith ⁵⁷, D. Smith ¹⁴³, K.M. Smith ⁵³, M. Smizanska ⁷¹,
 K. Smolek ¹²⁷, A.A. Snesarev ⁹⁴, S.W. Snow ⁸², J. Snow ¹¹¹, S. Snyder ²⁴, R. Sobie ^{169,k}, J. Sodomka ¹²⁷,
 A. Soffer ¹⁵³, C.A. Solans ¹⁶⁷, M. Solar ¹²⁷, J. Solc ¹²⁷, E.Yu. Soldatov ⁹⁶, U. Soldevila ¹⁶⁷,
 E. Solfaroli Camillocci ^{132a,132b}, A.A. Solodkov ¹²⁸, O.V. Solovyanov ¹²⁸, N. Soni ², V. Sopko ¹²⁷,
 B. Sopko ¹²⁷, M. Sosebee ⁷, R. Soualah ^{164a,164c}, A. Soukharev ¹⁰⁷, S. Spagnolo ^{72a,72b}, F. Spanò ⁷⁶,
 R. Spighi ^{19a}, G. Spigo ²⁹, F. Spila ^{132a,132b}, R. Spiwoks ²⁹, M. Spousta ¹²⁶, T. Spreitzer ¹⁵⁸, B. Spurlock ⁷,
 R.D. St. Denis ⁵³, J. Stahlman ¹²⁰, R. Stamen ^{58a}, E. Stanecka ³⁸, R.W. Stanek ⁵, C. Stanescu ^{134a},
 M. Stanescu-Bellu ⁴¹, S. Stapnes ¹¹⁷, E.A. Starchenko ¹²⁸, J. Stark ⁵⁵, P. Staroba ¹²⁵, P. Starovoitov ⁴¹,
 R. Staszewski ³⁸, A. Staude ⁹⁸, P. Stavina ^{144a}, G. Steele ⁵³, P. Steinbach ⁴³, P. Steinberg ²⁴, I. Stekl ¹²⁷,
 B. Stelzer ¹⁴², H.J. Stelzer ⁸⁸, O. Stelzer-Chilton ^{159a}, H. Stenzel ⁵², S. Stern ⁹⁹, G.A. Stewart ²⁹,
 J.A. Stillings ²⁰, M.C. Stockton ⁸⁵, K. Stoerig ⁴⁸, G. Stoica ^{25a}, S. Stonjek ⁹⁹, P. Strachota ¹²⁶, A.R. Stradling ⁷,
 A. Straessner ⁴³, J. Strandberg ¹⁴⁷, S. Strandberg ^{146a,146b}, A. Strandlie ¹¹⁷, M. Strang ¹⁰⁹, E. Strauss ¹⁴³,
 M. Strauss ¹¹¹, P. Strizenec ^{144b}, R. Ströhmer ¹⁷⁴, D.M. Strom ¹¹⁴, J.A. Strong ^{76,*}, R. Stroynowski ³⁹,
 J. Strube ¹²⁹, B. Stugu ¹³, I. Stumer ^{24,*}, J. Stupak ¹⁴⁸, P. Sturm ¹⁷⁵, N.A. Styles ⁴¹, D.A. Soh ^{151,w}, D. Su ¹⁴³,
 HS. Subramania ², A. Succurro ¹¹, Y. Sugaya ¹¹⁶, C. Suhr ¹⁰⁶, M. Suk ¹²⁶, V.V. Sulin ⁹⁴, S. Sultansoy ^{3d},
 T. Sumida ⁶⁷, X. Sun ⁵⁵, J.E. Sundermann ⁴⁸, K. Surulliz ¹³⁹, G. Susinno ^{36a,36b}, M.R. Sutton ¹⁴⁹, Y. Suzuki ⁶⁵,
 Y. Suzuki ⁶⁶, M. Svatos ¹²⁵, S. Swedish ¹⁶⁸, I. Sykora ^{144a}, T. Sykora ¹²⁶, J. Sánchez ¹⁶⁷, D. Ta ¹⁰⁵,
 K. Tackmann ⁴¹, A. Taffard ¹⁶³, R. Tafirout ^{159a}, N. Taiblum ¹⁵³, Y. Takahashi ¹⁰¹, H. Takai ²⁴,
 R. Takashima ⁶⁸, H. Takeda ⁶⁶, T. Takeshita ¹⁴⁰, Y. Takubo ⁶⁵, M. Talby ⁸³, A. Talyshiev ^{107,f}, M.C. Tamsett ²⁴,
 J. Tanaka ¹⁵⁵, R. Tanaka ¹¹⁵, S. Tanaka ¹³¹, S. Tanaka ⁶⁵, A.J. Tanasijczuk ¹⁴², K. Tani ⁶⁶, N. Tannoury ⁸³,
 S. Tapprogge ⁸¹, D. Tardif ¹⁵⁸, S. Tarem ¹⁵², F. Tarrade ²⁸, G.F. Tartarelli ^{89a}, P. Tas ¹²⁶, M. Tasevsky ¹²⁵,
 E. Tassi ^{36a,36b}, M. Tatarkhanov ¹⁴, Y. Tayalati ^{135d}, C. Taylor ⁷⁷, F.E. Taylor ⁹², G.N. Taylor ⁸⁶, W. Taylor ^{159b},
 M. Teinturier ¹¹⁵, M. Teixeira Dias Castanheira ⁷⁵, P. Teixeira-Dias ⁷⁶, K.K. Temming ⁴⁸, H. Ten Kate ²⁹,
 P.K. Teng ¹⁵¹, S. Terada ⁶⁵, K. Terashi ¹⁵⁵, J. Terron ⁸⁰, M. Testa ⁴⁷, R.J. Teuscher ^{158,k}, J. Therhaag ²⁰,
 T. Theveneaux-Pelzer ⁷⁸, S. Thoma ⁴⁸, J.P. Thomas ¹⁷, E.N. Thompson ³⁴, P.D. Thompson ¹⁷,
 P.D. Thompson ¹⁵⁸, A.S. Thompson ⁵³, L.A. Thomsen ³⁵, E. Thomson ¹²⁰, M. Thomson ²⁷, R.P. Thun ⁸⁷,
 F. Tian ³⁴, M.J. Tibbetts ¹⁴, T. Tic ¹²⁵, V.O. Tikhomirov ⁹⁴, Y.A. Tikhonov ^{107,f}, S. Timoshenko ⁹⁶,
 P. Tipton ¹⁷⁶, F.J. Tique Aires Viegas ²⁹, S. Tisserant ⁸³, T. Todorov ⁴, S. Todorova-Nova ¹⁶¹, B. Toggerson ¹⁶³,
 J. Tojo ⁶⁹, S. Tokár ^{144a}, K. Tokushuku ⁶⁵, K. Tollefson ⁸⁸, M. Tomoto ¹⁰¹, L. Tompkins ³⁰, K. Toms ¹⁰³,
 A. Tonoyan ¹³, C. Topfel ¹⁶, N.D. Topilin ⁶⁴, I. Torchiani ²⁹, E. Torrence ¹¹⁴, H. Torres ⁷⁸, E. Torró Pastor ¹⁶⁷,
 J. Toth ^{83,ad}, F. Touchard ⁸³, D.R. Tovey ¹³⁹, T. Trefzger ¹⁷⁴, L. Tremblet ²⁹, A. Tricoli ²⁹, I.M. Trigger ^{159a},
 S. Trincaz-Duvold ⁷⁸, M.F. Tripiana ⁷⁰, W. Trischuk ¹⁵⁸, B. Trocmé ⁵⁵, C. Troncon ^{89a},
 M. Trottier-McDonald ¹⁴², M. Trzebinski ³⁸, A. Trzupek ³⁸, C. Tsarouchas ²⁹, J.C.-L. Tseng ¹¹⁸,
 M. Tsiakiris ¹⁰⁵, P.V. Tsiareshka ⁹⁰, D. Tsionou ^{4,ag}, G. Tsipolitis ⁹, S. Tsiskaridze ¹¹, V. Tsiskaridze ⁴⁸,
 E.G. Tskhadadze ^{51a}, I.I. Tsukerman ⁹⁵, V. Tsulaia ¹⁴, J.-W. Tsung ²⁰, S. Tsuno ⁶⁵, D. Tsybychev ¹⁴⁸,
 A. Tua ¹³⁹, A. Tudorache ^{25a}, V. Tudorache ^{25a}, J.M. Tuggle ³⁰, M. Turala ³⁸, D. Turecek ¹²⁷, I. Turk Cakir ^{3e},
 E. Turlay ¹⁰⁵, R. Turra ^{89a,89b}, P.M. Tuts ³⁴, A. Tykhanov ⁷⁴, M. Tylmad ^{146a,146b}, M. Tyndel ¹²⁹,
 G. Tzanakos ⁸, K. Uchida ²⁰, I. Ueda ¹⁵⁵, R. Ueno ²⁸, M. Ugland ¹³, M. Uhlenbrock ²⁰, M. Uhrmacher ⁵⁴,
 F. Ukegawa ¹⁶⁰, G. Unal ²⁹, A. Undrus ²⁴, G. Unel ¹⁶³, Y. Unno ⁶⁵, D. Urbaniec ³⁴, G. Usai ⁷,
 M. Uslenghi ^{119a,119b}, L. Vacavant ⁸³, V. Vacek ¹²⁷, B. Vachon ⁸⁵, S. Vahsen ¹⁴, J. Valenta ¹²⁵, P. Valente ^{132a},
 S. Valentinetto ^{19a,19b}, A. Valero ¹⁶⁷, S. Valkar ¹²⁶, E. Valladoloid Gallego ¹⁶⁷, S. Vallecorsa ¹⁵²,
 J.A. Valls Ferrer ¹⁶⁷, H. van der Graaf ¹⁰⁵, E. van der Kraaij ¹⁰⁵, R. Van Der Leeuw ¹⁰⁵, E. van der Poel ¹⁰⁵,
 D. van der Ster ²⁹, N. van Eldik ²⁹, P. van Gemmeren ⁵, I. van Vulpen ¹⁰⁵, M. Vanadia ⁹⁹, W. Vandelli ²⁹,
 A. Vaniachine ⁵, P. Vankov ⁴¹, F. Vannucci ⁷⁸, R. Vari ^{132a}, T. Varol ⁸⁴, D. Varouchas ¹⁴, A. Vartapetian ⁷,
 K.E. Varvell ¹⁵⁰, V.I. Vassilakopoulos ⁵⁶, F. Vazeille ³³, T. Vazquez Schroeder ⁵⁴, G. Vegni ^{89a,89b},
 J.J. Veillet ¹¹⁵, F. Veloso ^{124a}, R. Veness ²⁹, S. Veneziano ^{132a}, A. Ventura ^{72a,72b}, D. Ventura ⁸⁴,
 M. Venturi ⁴⁸, N. Venturi ¹⁵⁸, V. Vercesi ^{119a}, M. Verducci ¹³⁸, W. Verkerke ¹⁰⁵, J.C. Vermeulen ¹⁰⁵,
 A. Vest ⁴³, M.C. Vetterli ^{142,d}, I. Vichou ¹⁶⁵, T. Vickey ^{145b,ah}, O.E. Vickey Boeriu ^{145b}, G.H.A. Viehhauser ¹¹⁸,
 S. Viel ¹⁶⁸, M. Villa ^{19a,19b}, M. Villaplana Perez ¹⁶⁷, E. Vilucchi ⁴⁷, M.G. Vincter ²⁸, E. Vinek ²⁹,
 V.B. Vinogradov ⁶⁴, M. Virchaux ^{136,*}, J. Virzi ¹⁴, O. Vitells ¹⁷², M. Viti ⁴¹, I. Vivarelli ⁴⁸, F. Vives Vaque ²,

S. Vlachos ⁹, D. Vladoiu ⁹⁸, M. Vlasak ¹²⁷, A. Vogel ²⁰, P. Vokac ¹²⁷, G. Volpi ⁴⁷, M. Volpi ⁸⁶, G. Volpini ^{89a}, H. von der Schmitt ⁹⁹, J. von Loeben ⁹⁹, H. von Radziewski ⁴⁸, E. von Toerne ²⁰, V. Vorobel ¹²⁶, V. Vorwerk ¹¹, M. Vos ¹⁶⁷, R. Voss ²⁹, T.T. Voss ¹⁷⁵, J.H. Vossebeld ⁷³, N. Vranjes ¹³⁶, M. Vranjes Milosavljevic ¹⁰⁵, V. Vrba ¹²⁵, M. Vreeswijk ¹⁰⁵, T. Vu Anh ⁴⁸, R. Vuillermet ²⁹, I. Vukotic ¹¹⁵, W. Wagner ¹⁷⁵, P. Wagner ¹²⁰, H. Wahlen ¹⁷⁵, S. Wahrmund ⁴³, J. Wakabayashi ¹⁰¹, S. Walch ⁸⁷, J. Walder ⁷¹, R. Walker ⁹⁸, W. Walkowiak ¹⁴¹, R. Wall ¹⁷⁶, P. Waller ⁷³, C. Wang ⁴⁴, H. Wang ¹⁷³, H. Wang ^{32b,ai}, J. Wang ¹⁵¹, J. Wang ⁵⁵, R. Wang ¹⁰³, S.M. Wang ¹⁵¹, T. Wang ²⁰, A. Warburton ⁸⁵, C.P. Ward ²⁷, M. Warsinsky ⁴⁸, A. Washbrook ⁴⁵, C. Wasicki ⁴¹, P.M. Watkins ¹⁷, A.T. Watson ¹⁷, I.J. Watson ¹⁵⁰, M.F. Watson ¹⁷, G. Watts ¹³⁸, S. Watts ⁸², A.T. Waugh ¹⁵⁰, B.M. Waugh ⁷⁷, M. Weber ¹²⁹, M.S. Weber ¹⁶, P. Weber ⁵⁴, A.R. Weidberg ¹¹⁸, P. Weigell ⁹⁹, J. Weingarten ⁵⁴, C. Weiser ⁴⁸, H. Wellenstein ²², P.S. Wells ²⁹, T. Wenaus ²⁴, D. Wendland ¹⁵, Z. Weng ^{151,w}, T. Wengler ²⁹, S. Wenig ²⁹, N. Wermes ²⁰, M. Werner ⁴⁸, P. Werner ²⁹, M. Werth ¹⁶³, M. Wessels ^{58a}, J. Wetter ¹⁶¹, C. Weydert ⁵⁵, K. Whalen ²⁸, S.J. Wheeler-Ellis ¹⁶³, A. White ⁷, M.J. White ⁸⁶, S. White ^{122a,122b}, S.R. Whitehead ¹¹⁸, D. Whiteson ¹⁶³, D. Whittington ⁶⁰, F. Wicek ¹¹⁵, D. Wicke ¹⁷⁵, F.J. Wickens ¹²⁹, W. Wiedenmann ¹⁷³, M. Wielers ¹²⁹, P. Wienemann ²⁰, C. Wiglesworth ⁷⁵, L.A.M. Wiik-Fuchs ⁴⁸, P.A. Wijeratne ⁷⁷, A. Wildauer ¹⁶⁷, M.A. Wildt ^{41,s}, I. Wilhelm ¹²⁶, H.G. Wilkens ²⁹, J.Z. Will ⁹⁸, E. Williams ³⁴, H.H. Williams ¹²⁰, W. Willis ³⁴, S. Willocq ⁸⁴, J.A. Wilson ¹⁷, M.G. Wilson ¹⁴³, A. Wilson ⁸⁷, I. Wingerter-Seez ⁴, S. Winkelmann ⁴⁸, F. Winklmeier ²⁹, M. Wittgen ¹⁴³, S.J. Wollstadt ⁸¹, M.W. Wolter ³⁸, H. Wolters ^{124a,h}, W.C. Wong ⁴⁰, G. Wooden ⁸⁷, B.K. Wosiek ³⁸, J. Wotschack ²⁹, M.J. Woudstra ⁸², K.W. Wozniak ³⁸, K. Wraight ⁵³, C. Wright ⁵³, M. Wright ⁵³, B. Wrona ⁷³, S.L. Wu ¹⁷³, X. Wu ⁴⁹, Y. Wu ^{32b,aj}, E. Wulf ³⁴, B.M. Wynne ⁴⁵, S. Xella ³⁵, M. Xiao ¹³⁶, S. Xie ⁴⁸, C. Xu ^{32b,z}, D. Xu ¹³⁹, B. Yabsley ¹⁵⁰, S. Yacoob ^{145b}, M. Yamada ⁶⁵, H. Yamaguchi ¹⁵⁵, A. Yamamoto ⁶⁵, K. Yamamoto ⁶³, S. Yamamoto ¹⁵⁵, T. Yamamura ¹⁵⁵, T. Yamanaka ¹⁵⁵, J. Yamaoka ⁴⁴, T. Yamazaki ¹⁵⁵, Y. Yamazaki ⁶⁶, Z. Yan ²¹, H. Yang ⁸⁷, U.K. Yang ⁸², Y. Yang ⁶⁰, Z. Yang ^{146a,146b}, S. Yanush ⁹¹, L. Yao ^{32a}, Y. Yao ¹⁴, Y. Yasu ⁶⁵, G.V. Ybeles Smit ¹³⁰, J. Ye ³⁹, S. Ye ²⁴, M. Yilmaz ^{3c}, R. Yoosoofmiya ¹²³, K. Yorita ¹⁷¹, R. Yoshida ⁵, C. Young ¹⁴³, C.J. Young ¹¹⁸, S. Youssef ²¹, D. Yu ²⁴, J. Yu ⁷, J. Yu ¹¹², L. Yuan ⁶⁶, A. Yurkewicz ¹⁰⁶, B. Zabinski ³⁸, R. Zaidan ⁶², A.M. Zaitsev ¹²⁸, Z. Zajacova ²⁹, L. Zanello ^{132a,132b}, A. Zaytsev ¹⁰⁷, C. Zeitnitz ¹⁷⁵, M. Zeman ¹²⁵, A. Zemla ³⁸, C. Zendler ²⁰, O. Zenin ¹²⁸, T. Ženiš ^{144a}, Z. Zinonos ^{122a,122b}, S. Zenz ¹⁴, D. Zerwas ¹¹⁵, G. Zevi della Porta ⁵⁷, Z. Zhan ^{32d}, D. Zhang ^{32b,ai}, H. Zhang ⁸⁸, J. Zhang ⁵, X. Zhang ^{32d}, Z. Zhang ¹¹⁵, L. Zhao ¹⁰⁸, T. Zhao ¹³⁸, Z. Zhao ^{32b}, A. Zhemchugov ⁶⁴, J. Zhong ¹¹⁸, B. Zhou ⁸⁷, N. Zhou ¹⁶³, Y. Zhou ¹⁵¹, C.G. Zhu ^{32d}, H. Zhu ⁴¹, J. Zhu ⁸⁷, Y. Zhu ^{32b}, X. Zhuang ⁹⁸, V. Zhuravlov ⁹⁹, D. Ziemińska ⁶⁰, N.I. Zimin ⁶⁴, R. Zimmermann ²⁰, S. Zimmermann ²⁰, S. Zimmermann ⁴⁸, M. Ziolkowski ¹⁴¹, R. Zitoun ⁴, L. Živković ³⁴, V.V. Zmouchko ^{128,*}, G. Zobernig ¹⁷³, A. Zoccoli ^{19a,19b}, M. zur Nedden ¹⁵, V. Zutshi ¹⁰⁶, L. Zwalinski ²⁹

¹ University at Albany, Albany, NY, United States² Department of Physics, University of Alberta, Edmonton, AB, Canada³ ^(a) Department of Physics, Ankara University, Ankara; ^(b) Department of Physics, Dumlupinar University, Kutahya; ^(c) Department of Physics, Gazi University, Ankara; ^(d) Division of Physics, TOBB University of Economics and Technology, Ankara; ^(e) Turkish Atomic Energy Authority, Ankara, Turkey⁴ LAPP, CNRS/IN2P3 and Université de Savoie, Annecy-le-Vieux, France⁵ High Energy Physics Division, Argonne National Laboratory, Argonne, IL, United States⁶ Department of Physics, University of Arizona, Tucson, AZ, United States⁷ Department of Physics, The University of Texas at Arlington, Arlington, TX, United States⁸ Physics Department, University of Athens, Athens, Greece⁹ Physics Department, National Technical University of Athens, Zografou, Greece¹⁰ Institute of Physics, Azerbaijan Academy of Sciences, Baku, Azerbaijan¹¹ Institut de Física d'Altes Energies and Departament de Física de la Universitat Autònoma de Barcelona and ICREA, Barcelona, Spain¹² ^(a) Institute of Physics, University of Belgrade, Belgrade; ^(b) Vinca Institute of Nuclear Sciences, University of Belgrade, Belgrade, Serbia¹³ Department for Physics and Technology, University of Bergen, Bergen, Norway¹⁴ Physics Division, Lawrence Berkeley National Laboratory and University of California, Berkeley, CA, United States¹⁵ Department of Physics, Humboldt University, Berlin, Germany¹⁶ Albert Einstein Center for Fundamental Physics and Laboratory for High Energy Physics, University of Bern, Bern, Switzerland¹⁷ School of Physics and Astronomy, University of Birmingham, Birmingham, United Kingdom¹⁸ ^(a) Department of Physics, Bogazici University, Istanbul; ^(b) Division of Physics, Dogus University, Istanbul; ^(c) Department of Physics Engineering, Gaziantep University, Gaziantep;^(d) Department of Physics, Istanbul Technical University, Istanbul, Turkey¹⁹ ^(a) INFN Sezione di Bologna; ^(b) Dipartimento di Fisica, Università di Bologna, Bologna, Italy²⁰ Physikalischs Institut, University of Bonn, Bonn, Germany²¹ Department of Physics, Boston University, Boston, MA, United States²² Department of Physics, Brandeis University, Waltham, MA, United States²³ ^(a) Universidade Federal do Rio De Janeiro COPPE/EE/IF, Rio de Janeiro; ^(b) Federal University of Juiz de Fora (UFJF), Juiz de Fora; ^(c) Federal University of Sao Joao del Rei (UFSJ), Sao Joao del Rei; ^(d) Instituto de Física, Universidade de São Paulo, São Paulo, Brazil²⁴ Physics Department, Brookhaven National Laboratory, Upton, NY, United States²⁵ ^(a) National Institute of Physics and Nuclear Engineering, Bucharest; ^(b) University Politehnica Bucharest, Bucharest; ^(c) West University in Timisoara, Timisoara, Romania

- ²⁶ Departamento de Física, Universidad de Buenos Aires, Buenos Aires, Argentina
²⁷ Cavendish Laboratory, University of Cambridge, Cambridge, United Kingdom
²⁸ Department of Physics, Carleton University, Ottawa, ON, Canada
²⁹ CERN, Geneva, Switzerland
³⁰ Enrico Fermi Institute, University of Chicago, Chicago, IL, United States
³¹ ^(a) Departamento de Física, Pontificia Universidad Católica de Chile, Santiago; ^(b) Departamento de Física, Universidad Técnica Federico Santa María, Valparaíso, Chile
³² ^(a) Institute of High Energy Physics, Chinese Academy of Sciences, Beijing; ^(b) Department of Modern Physics, University of Science and Technology of China, Anhui; ^(c) Department of Physics, Nanjing University, Jiangsu; ^(d) School of Physics, Shandong University, Shandong, China
³³ Laboratoire de Physique Corpusculaire, Clermont Université and Université Blaise Pascal and CNRS/IN2P3, Aubière Cedex, France
³⁴ Nevis Laboratory, Columbia University, Irvington, NY, United States
³⁵ Niels Bohr Institute, University of Copenhagen, Copenhagen, Denmark
³⁶ ^(a) INFN Gruppo Collegato di Cosenza; ^(b) Dipartimento di Fisica, Università della Calabria, Arcavate di Rende, Italy
³⁷ AGH University of Science and Technology, Faculty of Physics and Applied Computer Science, Krakow, Poland
³⁸ The Henryk Niewodniczanski Institute of Nuclear Physics, Polish Academy of Sciences, Krakow, Poland
³⁹ Physics Department, Southern Methodist University, Dallas, TX, United States
⁴⁰ Physics Department, University of Texas at Dallas, Richardson, TX, United States
⁴¹ DESY, Hamburg and Zeuthen, Germany
⁴² Institut für Experimentelle Physik IV, Technische Universität Dortmund, Dortmund, Germany
⁴³ Institut für Kern- und Teilchenphysik, Technical University Dresden, Dresden, Germany
⁴⁴ Department of Physics, Duke University, Durham, NC, United States
⁴⁵ SUPA – School of Physics and Astronomy, University of Edinburgh, Edinburgh, United Kingdom
⁴⁶ Fachhochschule Wiener Neustadt, Johannes Gutenbergstrasse 3, 2700 Wiener Neustadt, Austria
⁴⁷ INFN Laboratori Nazionali di Frascati, Frascati, Italy
⁴⁸ Fakultät für Mathematik und Physik, Albert-Ludwigs-Universität, Freiburg i.Br., Germany
⁴⁹ Section de Physique, Université de Genève, Geneva, Switzerland
⁵⁰ ^(a) INFN Sezione di Genova; ^(b) Dipartimento di Fisica, Università di Genova, Genova, Italy
⁵¹ ^(a) E. Andronikashvili Institute of Physics, Tbilisi State University, Tbilisi; ^(b) High Energy Physics Institute, Tbilisi State University, Tbilisi, Georgia
⁵² II Physikalisches Institut, Justus-Liebig-Universität Giessen, Giessen, Germany
⁵³ SUPA – School of Physics and Astronomy, University of Glasgow, Glasgow, United Kingdom
⁵⁴ II Physikalisches Institut, Georg-August-Universität, Göttingen, Germany
⁵⁵ Laboratoire de Physique Subatomique et de Cosmologie, Université Joseph Fourier and CNRS/IN2P3 and Institut National Polytechnique de Grenoble, Grenoble, France
⁵⁶ Department of Physics, Hampton University, Hampton, VA, United States
⁵⁷ Laboratory for Particle Physics and Cosmology, Harvard University, Cambridge, MA, United States
⁵⁸ ^(a) Kirchhoff-Institut für Physik, Ruprecht-Karls-Universität Heidelberg, Heidelberg; ^(b) Physikalisches Institut, Ruprecht-Karls-Universität Heidelberg, Heidelberg; ^(c) ZITI Institut für technische Informatik, Ruprecht-Karls-Universität Heidelberg, Mannheim, Germany
⁵⁹ Faculty of Applied Information Science, Hiroshima Institute of Technology, Hiroshima, Japan
⁶⁰ Department of Physics, Indiana University, Bloomington, IN, United States
⁶¹ Institut für Astro- und Teilchenphysik, Leopold-Franzens-Universität, Innsbruck, Austria
⁶² University of Iowa, Iowa City, IA, United States
⁶³ Department of Physics and Astronomy, Iowa State University, Ames, IA, United States
⁶⁴ Joint Institute for Nuclear Research, JINR Dubna, Dubna, Russia
⁶⁵ KEK, High Energy Accelerator Research Organization, Tsukuba, Japan
⁶⁶ Graduate School of Science, Kobe University, Kobe, Japan
⁶⁷ Faculty of Science, Kyoto University, Kyoto, Japan
⁶⁸ Kyoto University of Education, Kyoto, Japan
⁶⁹ Department of Physics, Kyushu University, Fukuoka, Japan
⁷⁰ Instituto de Física La Plata, Universidad Nacional de La Plata and CONICET, La Plata, Argentina
⁷¹ Physics Department, Lancaster University, Lancaster, United Kingdom
⁷² ^(a) INFN Sezione di Lecce; ^(b) Dipartimento di Matematica e Fisica, Università del Salento, Lecce, Italy
⁷³ Oliver Lodge Laboratory, University of Liverpool, Liverpool, United Kingdom
⁷⁴ Department of Physics, Jožef Stefan Institute and University of Ljubljana, Ljubljana, Slovenia
⁷⁵ School of Physics and Astronomy, Queen Mary University of London, London, United Kingdom
⁷⁶ Department of Physics, Royal Holloway University of London, Surrey, United Kingdom
⁷⁷ Department of Physics and Astronomy, University College London, London, United Kingdom
⁷⁸ Laboratoire de Physique Nucléaire et de Hautes Energies, UPMC and Université Paris-Diderot and CNRS/IN2P3, Paris, France
⁷⁹ Fysiska institutionen, Lunds universitet, Lund, Sweden
⁸⁰ Departamento de Física Teórica C-15, Universidad Autónoma de Madrid, Madrid, Spain
⁸¹ Institut für Physik, Universität Mainz, Mainz, Germany
⁸² School of Physics and Astronomy, University of Manchester, Manchester, United Kingdom
⁸³ CPPM, Aix-Marseille Université and CNRS/IN2P3, Marseille, France
⁸⁴ Department of Physics, University of Massachusetts, Amherst, MA, United States
⁸⁵ Department of Physics, McGill University, Montreal, QC, Canada
⁸⁶ School of Physics, University of Melbourne, Victoria, Australia
⁸⁷ Department of Physics, The University of Michigan, Ann Arbor, MI, United States
⁸⁸ Department of Physics and Astronomy, Michigan State University, East Lansing, MI, United States
⁸⁹ ^(a) INFN Sezione di Milano; ^(b) Dipartimento di Fisica, Università di Milano, Milano, Italy
⁹⁰ B.I. Stepanov Institute of Physics, National Academy of Sciences of Belarus, Minsk, Belarus
⁹¹ National Scientific and Educational Centre for Particle and High Energy Physics, Minsk, Belarus
⁹² Department of Physics, Massachusetts Institute of Technology, Cambridge, MA, United States
⁹³ Group of Particle Physics, University of Montreal, Montreal, QC, Canada
⁹⁴ P.N. Lebedev Institute of Physics, Academy of Sciences, Moscow, Russia
⁹⁵ Institute for Theoretical and Experimental Physics (ITEP), Moscow, Russia
⁹⁶ Moscow Engineering and Physics Institute (MEPhI), Moscow, Russia
⁹⁷ Skobeltsyn Institute of Nuclear Physics, Lomonosov Moscow State University, Moscow, Russia
⁹⁸ Fakultät für Physik, Ludwig-Maximilians-Universität München, München, Germany
⁹⁹ Max-Planck-Institut für Physik (Werner-Heisenberg-Institut), München, Germany
¹⁰⁰ Nagasaki Institute of Applied Science, Nagasaki, Japan
¹⁰¹ Graduate School of Science and Kobayashi-Maskawa Institute, Nagoya University, Nagoya, Japan
¹⁰² ^(a) INFN Sezione di Napoli; ^(b) Dipartimento di Scienze Fisiche, Università di Napoli, Napoli, Italy

- 103 Department of Physics and Astronomy, University of New Mexico, Albuquerque, NM, United States
 104 Institute for Mathematics, Astrophysics and Particle Physics, Radboud University Nijmegen/Nikhef, Nijmegen, Netherlands
 105 Nikhef National Institute for Subatomic Physics and University of Amsterdam, Amsterdam, Netherlands
 106 Department of Physics, Northern Illinois University, DeKalb, IL, United States
 107 Budker Institute of Nuclear Physics, SB RAS, Novosibirsk, Russia
 108 Department of Physics, New York University, New York, NY, United States
 109 Ohio State University, Columbus, OH, United States
 110 Faculty of Science, Okayama University, Okayama, Japan
 111 Horner L. Dodge Department of Physics and Astronomy, University of Oklahoma, Norman, OK, United States
 112 Department of Physics, Oklahoma State University, Stillwater, OK, United States
 113 Palacký University, RCPIM, Olomouc, Czech Republic
 114 Center for High Energy Physics, University of Oregon, Eugene, OR, United States
 115 LAL, Université Paris-Sud and CNRS/IN2P3, Orsay, France
 116 Graduate School of Science, Osaka University, Osaka, Japan
 117 Department of Physics, University of Oslo, Oslo, Norway
 118 Department of Physics, Oxford University, Oxford, United Kingdom
 119 ^(a) INFN Sezione di Pavia; ^(b) Dipartimento di Fisica, Università di Pavia, Pavia, Italy
 120 Department of Physics, University of Pennsylvania, Philadelphia, PA, United States
 121 Petersburg Nuclear Physics Institute, Gatchina, Russia
 122 ^(a) INFN Sezione di Pisa; ^(b) Dipartimento di Fisica E. Fermi, Università di Pisa, Pisa, Italy
 123 Department of Physics and Astronomy, University of Pittsburgh, Pittsburgh, PA, United States
 124 ^(a) Laboratorio de Instrumentacion e Física Experimental de Partículas – LIP, Lisboa, Portugal; ^(b) Departamento de Física Teórica y del Cosmos and CAFPE, Universidad de Granada, Granada, Spain
 125 Institute of Physics, Academy of Sciences of the Czech Republic, Praha, Czech Republic
 126 Faculty of Mathematics and Physics, Charles University in Prague, Praha, Czech Republic
 127 Czech Technical University in Prague, Praha, Czech Republic
 128 State Research Center Institute for High Energy Physics, Protvino, Russia
 129 Particle Physics Department, Rutherford Appleton Laboratory, Didcot, United Kingdom
 130 Physics Department, University of Regina, Regina, SK, Canada
 131 Ritsumeikan University, Kusatsu, Shiga, Japan
 132 ^(a) INFN Sezione di Roma I; ^(b) Dipartimento di Fisica, Università La Sapienza, Roma, Italy
 133 ^(a) INFN Sezione di Roma Tor Vergata; ^(b) Dipartimento di Fisica, Università di Roma Tor Vergata, Roma, Italy
 134 ^(a) INFN Sezione di Roma Tre; ^(b) Dipartimento di Fisica, Università Roma Tre, Roma, Italy
 135 ^(a) Faculté des Sciences Ain Chock, Réseau Universitaire de Physique des Hautes Energies – Université Hassan II, Casablanca; ^(b) Centre National de l'Energie des Sciences Techniques Nucléaires, Rabat; ^(c) Faculté des Sciences Semlalia, Université Cadi Ayyad, LPHEA, Marrakech; ^(d) Faculté des Sciences, Université Mohamed Premier and LPTPM, Oujda; ^(e) Faculté des Sciences, Université Mohammed V-Agdal, Rabat, Morocco
 136 DSM/IRFU (Institut de Recherches sur les Lois Fondamentales de l'Univers), CEA Saclay (Commissariat à l'Energie Atomique), Gif-sur-Yvette, France
 137 Santa Cruz Institute for Particle Physics, University of California Santa Cruz, Santa Cruz, CA, United States
 138 Department of Physics, University of Washington, Seattle, WA, United States
 139 Department of Physics and Astronomy, University of Sheffield, Sheffield, United Kingdom
 140 Department of Physics, Shinshu University, Nagano, Japan
 141 Fachbereich Physik, Universität Siegen, Siegen, Germany
 142 Department of Physics, Simon Fraser University, Burnaby, BC, Canada
 143 SLAC National Accelerator Laboratory, Stanford, CA, United States
 144 ^(a) Faculty of Mathematics, Physics & Informatics, Comenius University, Bratislava; ^(b) Department of Subnuclear Physics, Institute of Experimental Physics of the Slovak Academy of Sciences, Kosice, Slovak Republic
 145 ^(a) Department of Physics, University of Johannesburg, Johannesburg; ^(b) School of Physics, University of the Witwatersrand, Johannesburg, South Africa
 146 ^(a) Department of Physics, Stockholm University; ^(b) The Oskar Klein Centre, Stockholm, Sweden
 147 Physics Department, Royal Institute of Technology, Stockholm, Sweden
 148 Departments of Physics & Astronomy and Chemistry, Stony Brook University, Stony Brook, NY, United States
 149 Department of Physics and Astronomy, University of Sussex, Brighton, United Kingdom
 150 School of Physics, University of Sydney, Sydney, Australia
 151 Institute of Physics, Academia Sinica, Taipei, Taiwan
 152 Department of Physics, Technion: Israel Institute of Technology, Haifa, Israel
 153 Raymond and Beverly Sackler School of Physics and Astronomy, Tel Aviv University, Tel Aviv, Israel
 154 Department of Physics, Aristotle University of Thessaloniki, Thessaloniki, Greece
 155 International Center for Elementary Particle Physics and Department of Physics, The University of Tokyo, Tokyo, Japan
 156 Graduate School of Science and Technology, Tokyo Metropolitan University, Tokyo, Japan
 157 Department of Physics, Tokyo Institute of Technology, Tokyo, Japan
 158 Department of Physics, University of Toronto, Toronto, ON, Canada
 159 ^(a) TRIUMF, Vancouver, BC; ^(b) Department of Physics and Astronomy, York University, Toronto, ON, Canada
 160 Institute of Pure and Applied Sciences, University of Tsukuba, 1-1 Tennodai, Tsukuba, Ibaraki 305-8571, Japan
 161 Science and Technology Center, Tufts University, Medford, MA, United States
 162 Centro de Investigaciones, Universidad Antonio Narino, Bogota, Colombia
 163 Department of Physics and Astronomy, University of California Irvine, Irvine, CA, United States
 164 ^(a) INFN Gruppo Collegato di Udine; ^(b) ICTP, Trieste; ^(c) Dipartimento di Chimica, Fisica e Ambiente, Università di Udine, Udine, Italy
 165 Department of Physics, University of Illinois, Urbana, IL, United States
 166 Department of Physics and Astronomy, University of Uppsala, Uppsala, Sweden
 167 Instituto de Física Corpuscular (IFIC) and Departamento de Física Atómica, Molecular y Nuclear and Departamento de Ingeniería Electrónica and Instituto de Microelectrónica de Barcelona (IMB-CNM), University of Valencia and CSIC, Valencia, Spain
 168 Department of Physics, University of British Columbia, Vancouver, BC, Canada
 169 Department of Physics and Astronomy, University of Victoria, Victoria, BC, Canada
 170 Department of Physics, University of Warwick, Coventry, United Kingdom
 171 Waseda University, Tokyo, Japan
 172 Department of Particle Physics, The Weizmann Institute of Science, Rehovot, Israel
 173 Department of Physics, University of Wisconsin, Madison, WI, United States
 174 Fakultät für Physik und Astronomie, Julius-Maximilians-Universität, Würzburg, Germany
 175 Fachbereich C Physik, Bergische Universität Wuppertal, Wuppertal, Germany
 176 Department of Physics, Yale University, New Haven, CT, United States

¹⁷⁷ Yerevan Physics Institute, Yerevan, Armenia¹⁷⁸ Domaine Scientifique de la Doua, Centre de Calcul CNRS/IN2P3, Villeurbanne Cedex, France

- ^a Also at Laboratorio de Instrumentacao e Fisica Experimental de Particulas – LIP, Lisboa, Portugal.
- ^b Also at Faculdade de Ciencias and CFNUL, Universidade de Lisboa, Lisboa, Portugal.
- ^c Also at Particle Physics Department, Rutherford Appleton Laboratory, Didcot, United Kingdom.
- ^d Also at TRIUMF, Vancouver, BC, Canada.
- ^e Also at Department of Physics, California State University, Fresno, CA, United States.
- ^f Also at Novosibirsk State University, Novosibirsk, Russia.
- ^g Also at Fermilab, Batavia, IL, United States.
- ^h Also at Department of Physics, University of Coimbra, Coimbra, Portugal.
- ⁱ Also at Department of Physics, UASLP, San Luis Potosi, Mexico.
- ^j Also at Università di Napoli Parthenope, Napoli, Italy.
- ^k Also at Institute of Particle Physics (IPP), Canada.
- ^l Also at Department of Physics, Middle East Technical University, Ankara, Turkey.
- ^m Also at Louisiana Tech University, Ruston, LA, United States.
- ⁿ Also at Dep. Fisica and CEFITEC of Faculdade de Ciencias e Tecnologia, Universidade Nova de Lisboa, Caparica, Portugal.
- ^o Also at Department of Physics and Astronomy, University College London, London, United Kingdom.
- ^p Also at Group of Particle Physics, University of Montreal, Montreal, QC, Canada.
- ^q Also at Department of Physics, University of Cape Town, Cape Town, South Africa.
- ^r Also at Institute of Physics, Azerbaijan Academy of Sciences, Baku, Azerbaijan.
- ^s Also at Institut für Experimentalphysik, Universität Hamburg, Hamburg, Germany.
- ^t Also at Manhattan College, New York, NY, United States.
- ^u Also at School of Physics, Shandong University, Shandong, China.
- ^v Also at CPPM, Aix-Marseille Université and CNRS/IN2P3, Marseille, France.
- ^w Also at School of Physics and Engineering, Sun Yat-sen University, Guangzhou, China.
- ^x Also at Academia Sinica Grid Computing, Institute of Physics, Academia Sinica, Taipei, Taiwan.
- ^y Also at INFN Sezione di Roma I, Italy.
- ^z Also at DSM/IRFU (Institut de Recherches sur les Lois Fondamentales de l'Univers), CEA Saclay (Commissariat à l'Energie Atomique), Gif-sur-Yvette, France.
- ^{aa} Also at Section de Physique, Université de Genève, Geneva, Switzerland.
- ^{ab} Also at Departamento de Fisica, Universidade de Minho, Braga, Portugal.
- ^{ac} Also at Department of Physics and Astronomy, University of South Carolina, Columbia, SC, United States.
- ^{ad} Also at Institute for Particle and Nuclear Physics, Wigner Research Centre for Physics, Budapest, Hungary.
- ^{ae} Also at California Institute of Technology, Pasadena, CA, United States.
- ^{af} Also at IAL, Université Paris-Sud and CNRS/IN2P3, Orsay, France.
- ^{ag} Also at Department of Physics and Astronomy, University of Sheffield, Sheffield, United Kingdom.
- ^{ah} Also at Department of Physics, Oxford University, Oxford, United Kingdom.
- ^{ai} Also at Institute of Physics, Academia Sinica, Taipei, Taiwan.
- ^{aj} Also at Department of Physics, The University of Michigan, Ann Arbor, MI, United States.
- * Deceased.